UNITED NATIONS UNIVERSITY
GEOTHERMAL TRAINING PROGRAMME
Orkustofnun, Grensasvegur 9,
IS-108 Reykjavik, Iceland

Reports 2012
Number 14

GEOPHYSICAL EXPLORATION OF HIGH-TEMPERATURE GEOTHERMAL AREAS USING RESISTIVITY METHODS – CASE STUDY: THEISTAREYKIR AREA, NE-ICELAND

Eriya Kahwa
Ministry of Energy and Mineral Development
Department of Geological Survey and Mines
P.O. Box 9, Entebbe
UGANDA
kahwaeriya@gmail.com

ABSTRACT

Measuring the electrical resistivity, ρ, of the subsurface is the most powerful geophysical prospecting method in high-temperature geothermal exploration and the main method used in delineating geothermal resources. Resistivity surveys using TEM and MT methods have been done in the Theistareykir geothermal area since 2004. In this work, sixteen TEM and MT soundings on two profiles were jointly inverted, based on 1D models. Cross-sections and iso-resistivity maps of the joint inversion models of the TEM and MT data from Theistareykir geothermal area, NE-Iceland reveal features similar to other high-temperature areas in Iceland, with a resistive zone reflecting unaltered rock formations, a shallow conductive cap and a resistive core reflecting chlorite-epidote alteration. Two deep conductors (<10 Ωm), possibly related to the heat source, were interpreted north of Bóndhólsskard and northeast of Stórihver. Good correlation between the subsurface resistivity and hydrothermal alteration in borehole ThG-05 was confirmed.

1. INTRODUCTION

Uganda is in advanced stages of surface exploration in the main areas of geothermal potential, Katwe, Kibiro and Buranga. However, shallow boreholes drilled to a depth of 200-300 m for temperature gradient measurements in Katwe and Kibiro indicated an average temperature gradient of only 30-36°C/km. The observed low-temperature gradient has been interpreted to suggest either a deep reservoir in Katwe and Kibiro or a geothermal reservoir offset from the drilled areas (Bahati, 2011). The author of this report was nominated for the six months geophysical exploration course so as to become acquainted with the principles, data collection, data processing and interpretation of TEM and MT data, which are the most probable geophysical techniques in delineating the existence, depth and extent of geothermal reservoirs in these priority areas.

Geophysical techniques or methods usually measure physical properties that are related to geothermal systems. To locate, quantify and map geothermal systems using geophysical methods, the system must have anomalous physical properties different from those of the surrounding rocks. The most important physical parameters measured in geothermal systems include: temperature, electrical resistivity, density, magnetisation, and seismic velocity.

The Theistareykir high-temperature geothermal area is located in NE-Iceland. The geothermal area has been the subject of surface exploration off and on for almost 40 years with the utilisation of geothermal energy for electricity production as a long term goal (Gautason et al., 2010). In this report, a total of sixteen TEM and MT soundings acquired from Theistareykir between 2009 and 2011 on two profiles were processed and 1D inverted. The results are presented as resistivity cross-sections and iso-resistivity maps. A description is given on data acquisition in the area, processing, joint-inversion of the data, discussion and comparison of resistivity results with hydrothermal alteration/borehole temperatures. Finally, conclusions and discussions are presented.

2. GEOPHYSICAL EXPLORATION METHODS FOR GEOTHERMAL RESOURCES

Geophysical exploration techniques are classified into two categories, depending on the measured parameters: direct methods and structural or indirect methods (Hersir and Björnsson, 1991). Direct methods give information on reservoir parameters that are influenced by geothermal activity while indirect/structural methods mostly reveal structures or geological bodies for the understanding of the geothermal system.

2.1 Direct methods

Surface temperature and thermal surveys: Thermal measurements are the most direct method for studying geothermal systems. Measurements are usually made in shallow holes but the most preferred technique is to conduct temperature surveys in wells that are at least 100 m deep. The objectives of thermal gradient surveys include: detecting areas of unusually high temperature and determining the component of heat flow along the direction of the borehole. Quantitative results are obtained when thermal gradients are converted to heat flow through the use of Fourier´s equation (Manzella, 2007):

$$\Delta T/\Delta z = \Phi z/K \quad (1)$$

where $\Delta T/\Delta z$ = Vertical temperature gradient (°C m^{-1});
Φz = Conductive heat flow density (W/m^2); and
K = Thermal conductivity (W/m°C)

Electrical methods: A number of electrical resistivity methods are deployed in geothermal exploration, based on the fact that temperature affects the electrical properties of rocks. However, temperature is not the only factor affecting the conductivity of rocks; an increase in the water content or total amount of dissolved solids can also increase conductivity by large amounts. Electromagnetic soundings determine variations in the electric conductivity of the earth with depth. Electromagnetic sounding methods include natural-field methods (e.g. magnetotellurics), and controlled source induction methods.

In magnetotellurics (MT), the natural electromagnetic field of the earth is used as an energy source to probe the subsurface. The natural electromagnetic field contains a wide spectrum of frequencies, including very low frequencies that can probe several tens of kilometres. The low frequencies are generated by ionospheric and magnetospheric currents that arise when plasma emitted from the sun interacts with the earth's magnetic field. One source of high frequency current fluctuations is an electric storm. Some of the thunderstorm energy is converted into electromagnetic fields, which are propagated in the ionosphere-earth interspace.

In the majority of systems, when carrying out magnetotellurics today, the five electromagnetic field components (E_x, E_y, H_x, H_y and H_z) are converted to digital form and later a spectral analysis is done. Once the various spectra have been calculated, they must be converted to apparent resistivity and phase as a function of frequency. It is assumed that at any given frequency there is a linear relationship between the electric field vector and the magnetic vector.

$$\boldsymbol{E} = \boldsymbol{Z}\,\boldsymbol{H} \quad (2)$$

where $\boldsymbol{H}$ = Magnetic field (gamma);
$\boldsymbol{E}$ = Electric field (mV/km); and
$\boldsymbol{Z}$ = Tensor determined by the resistivity structure and frequency.

In electromagnetic (EM) methods, an artificial source is used to generate an electromagnetic field. EM soundings consist of measurements at a number of frequencies, using a fixed source and receiver. The distribution of currents induced in the earth depends on the product of electrical conductivity, magnetic permeability and frequency. Since low-frequency currents diffuse to greater depths than high-frequency currents, measurements of EM response at several frequencies contain information on the variation of conductivity with depth.

EM sounding methods have advantages over natural-source sounding (e.g. magnetotellurics) since they provide better resolution and are less easily distorted by lateral variations in the resistivity, commonly referred to as the static shift.

Self-potential or spontaneous polarization surveys involve the measurement of naturally existing voltage gradients in the earth which have a variety of causes, including oxidation and the reduction of various minerals by reaction with groundwater, and streaming potentials which occur when fresh water is forced to move through a fine pore structure, stripping ions from the walls of the pores. In areas with strong geothermally related self-potential anomalies, variations of as much as several volts can be observed over distances from a few hundred metres up to a few kilometres.

2.2 Structural/indirect methods

Gravity surveys: These are used in geothermal exploration to define lateral density variations, which may be related to a deep magmatic body, which may represent the heat source. These anomalies can be created by differentiation of magma or variation in the depth of the crust-mantle interface which also creates depth variation of isotherms.

Magnetic surveys: The magnetic method is useful in mapping near-surface volcanic rocks that are often of interest in geothermal exploration, but the greatest potential for the method lies in its ability to detect the depth at which the Curie temperature is reached. The ability to determine the depth to the Curie point would be an ability to determine the depth to the Curie point isotherm as well (Manzella, 2007).

3. RESISTIVITY

Resistivity is one of the most useful geophysical parameters in searching for geothermal resources. As better and deeper imaging of the resistivity structure of geothermal systems has become possible with the use of methods such as MT surveying, it has been shown that the lowest resistivity is usually in a zone above the reservoir and the resistivity of the actual reservoir can be much higher (Ussher et al., 2000).

3.1 Resistivity of rocks

The resistivity of rocks has been described by a number of authors and this particular chapter is based on the description by Hersir and Árnason (2009) and Flóvenz et al. (2012). The specific resistivity, ρ, is defined by Ohms's law. The electrical field, $\boldsymbol{E}$ (V/m) at a point in a material is proportional to the current density, $\boldsymbol{j}$ (A/m^2):

$$\boldsymbol{E} = \rho \boldsymbol{j} \tag{3}$$

The proportionality constant, ρ, depends on the material and is called the (specific) resistivity, and it is measured in Ωm. The reciprocal of resistivity is conductivity, $\sigma = \rho^{-1}$. Electrical conductivity in minerals and solutions takes place by the movement of electrons and ions. Most rocks near the earth´s surface have low conductivity. Conduction of electricity is mostly through groundwater contained in pores of the rocks and along surface layers at the contact of rocks and solution.

3.1.1 Factors affecting electrical resistivity of water-bearing rocks

The electrical resistivity of rocks is mainly influenced by the following parameters (Hersir and Árnason, 2009):

- Porosity and the pore structure of the rock;
- Amount of water (saturation);
- Salinity of the water;
- Temperature;
- Water-rock interaction and alteration;
- Pressure;
- Steam content in the water.

The most important factors are porosity, temperature, salinity and water-rock interaction. In geothermal areas, the rocks are water-saturated. Ionic conduction in the saturating fluid depends on the number and mobility of ions in addition to the connectivity of the flow paths of the rock matrix.

Porosity and the pore structure of the rock: Porosity, φ_t, of a material is defined as the ratio of the pore volume to the total volume of the rock, given by the formula:

$$\varphi_t = \frac{V_\varphi}{V} \tag{4}$$

where φ_t = Fractional porosity;
V_φ = Volume of pores; and
V = Total volume of the rock.

The degree of saturation and the porosity is of great importance to the bulk resistivity of the rock. The following empirical equation, commonly referred to as Archie's law, describes how resistivity depends on porosity if ionic conduction dominates other conduction mechanisms in the rock (Archie, 1942; Hersir and Björnsson, 1991). Equation 5 is valid if the resistivity of the pore fluid is ≤ 2 Ωm:

$$\rho = \rho_w \alpha \varphi_t^{-n} = \rho_w F \tag{5}$$

where ρ = Bulk resistivity;
ρ_w = Resistivity of the pore fluid;
φ_t = Fractional porosity;
α = Empirical parameter describing the type of porosity, varying from less than 1 for inter-granular porosity, to more than 1 for joint porosity, but is usually around 1;
n = Cementation factor, usually ~1-2;
F = Formation factor, $F = \alpha \varphi_t^{-n}$.

The salinity of the water (fluid) present in the pore space of the rock affects the resistivity of the bulk rock. An increase in the amounts of dissolved solids in the pore fluid can increase the conductivity by large amounts (Figure 1). Considering water as an electrolyte, the conductivity of an electrolyte solution can be expressed by:

$$\sigma = \frac{1}{\rho} = F(c_1 q_1 m_1 + c_2 q_2 m_2 + \cdots) \qquad (6)$$

where σ = Conductivity (S/m);
F = Faraday's constant (9.649×10^4 C/mol);
c_i = Concentration of ions;
q_i = Valence of ions;
m_i = Mobility of ions.

Temperature: The resistivity of aqueous solutions has been observed to decrease with increasing temperature due to an increase in ion mobility caused by a decrease in the viscosity of the water. This is usually evident at moderate temperatures between 0 and 200°C (Figure 2). Dakhnov (1962) described this relationship as:

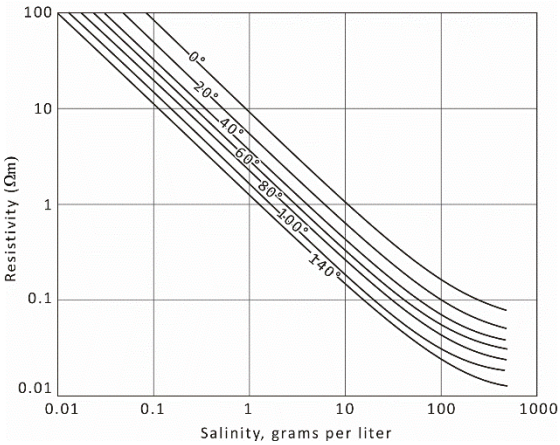

FIGURE 1: The resistivity of solutions of sodium chloride as a function of concentration and temperature (Flóvenz et al., 2012, based on Keller and Frischknecht, 1966)

$$\rho_w = \frac{\rho_{wo}}{1 + \alpha\,(T - T_O)} \qquad (7)$$

where ρ_w = Resistivity of the fluid at temperature T (Ωm);
ρ_{wo} = Resistivity of the fluid at reference temperature T_0 (Ωm);
α = Temperature coefficient of resistivity (°C); $\alpha \approx 0.023°C^{-1}$ for $T_0 = 25°C$;
T = Temperature (°C);
T_o = Reference temperature (°C).

At high temperatures, there is a decrease in the dielectric permittivity of water, resulting in a decrease in the number of dissociated ions in the solution. At temperatures above 300°C, fluid resistivity starts to increase, as shown in Figure 2.

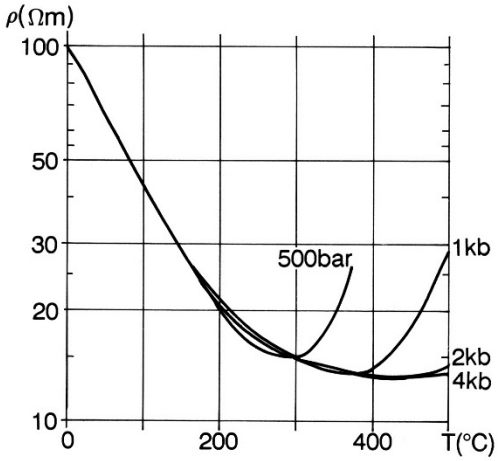

FIGURE 2: The resistivity of solutions of NaCl as a function of temperature at different pressures (Flóvenz et al., 2012, based on Quist and Marshall, 1966)

Water-rock interaction and alteration: The distribution of alteration minerals provides information on the temperature of the geothermal system and the flow path of the geothermal water. The alteration intensity is normally low for temperatures below 50-100°C. At temperatures between 100 and 220°C, low-temperature zeolites and clay mineral smectite are formed (Árnason et al., 2000). The range where low-temperature zeolites and smectite are abundant is referred to as the smectite-zeolite zone. Between 220 and 250°C, the low-temperature zeolites disappear and the smectite is transformed into chlorite in the so called mixed-layer clay zone. At higher temperatures, 260-270°C, epidote becomes abundant in the chlorite-epidote zone. This zoning applies for fresh water basaltic systems; however, in brine systems, the zoning is similar but the mixed-layer clay zone extends over a wider temperature range to a magnitude of 250-300°C (Árnason et al., 2000).

Resistivity in high-temperature geothermal areas would be expected to decrease with increasing temperature. However, in high-temperature geothermal areas, the resistivity in the chlorite and chlorite-epidote alteration zone increases due to an extremely low concentration of mobile cations (Figure 3). Chlorite alteration is usually expected at depths where resistivity increases with temperatures of 250°C or higher, provided the alteration is in equilibrium with the temperature. If the geothermal system has

cooled, the alteration remains the same and, thus, the resistivity structure is similar. In such a case, the interpretation of the resistivity structure can be misleading, since it reflects alteration minerals that were formed in the past (Hersir and Árnason, 2009).

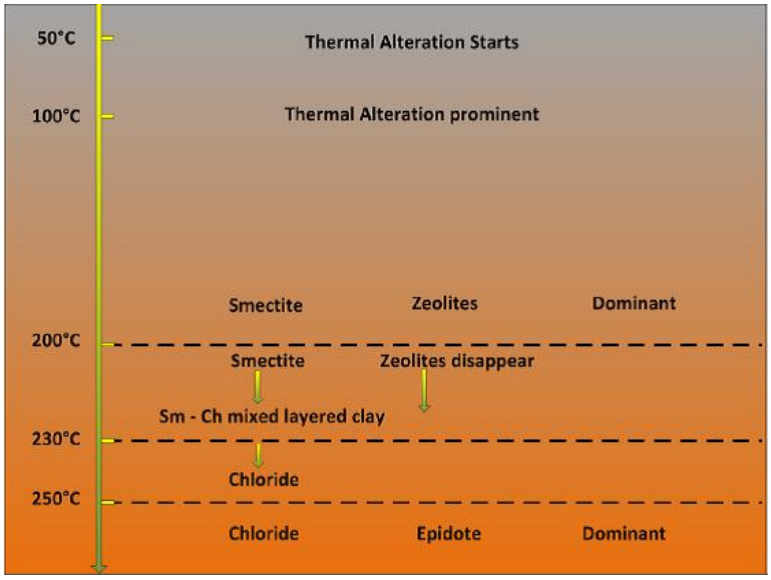

FIGURE 3: Alteration mineralogy and temperature (Hersir, 2012)

3.2 Transient-electromagnetics (TEM)

The transient-electromagnetic method (TEM), like any other electromagnetic method, is based on the fact that the magnetic field (primary) varies and, according to the Maxwell's equations, induces an electrical current into the surroundings. The associated electrical and magnetic fields are called the secondary fields.

The TEM method uses an ungrounded loop as a transmitter coil. The current in the coil is abruptly turned off (Figure 4), and the rate of change of the secondary field due to induced eddy currents in the ground is measured in the receiver coil. The depicted waveform is often referred to as a square waveform. The datasets are recorded in decay-time-windows called gates. The gates are arranged with a logarithmically increasing width to improve the signal/noise ratio, especially at late-times.

The current distribution and the decay rate of the secondary magnetic field depend on the resistivity structure of the earth. The decay rate, recorded as a function of time after the current turn-off, can be interpreted in terms of the subsurface resistivity structure. The depth of penetration in the central loop depends on how long the induction in the receiver coil can be traced in time before it is drowned in noise.

The apparent resistivity $\rho_a(r, t)$, in terms of the induced voltage at late times after the source current is turned off, is defined by:

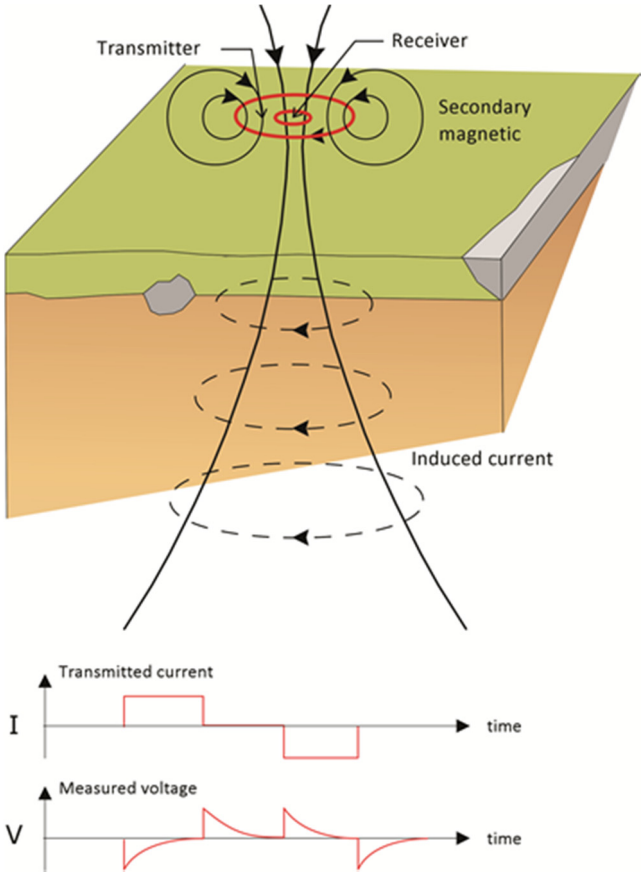

FIGURE 4: TEM sounding setup; the receiver coil is in the centre of the transmitter loop; transmitted current and measured transient voltage are shown as well (Flóvenz et al., 2012)

$$\rho_a(r,t) = \frac{\mu_o}{4\pi}\left[\frac{2\mu_o A_r n_r A_s n_s I_0}{5t^{5/2} v(r,t)}\right]^{2/3} \quad (8)$$

where μ_o = Magnetic permeability in vacuum (H/m);
A_r = Cross-sectional area of the receiver (m^2);
A_s = Cross-sectional area of transmitter (m^2);
n_r = Number of windings in the receiver coil;
I_0 = Current strength (A);
n_s = Number of windings in the transmitter loop;
t = Time elapsed after the transmitter current is turned off (s);
$v(r,t)$ = Transient voltage (V);
r = Radius of the transmitter loop (m).

3.3 Magnetotellurics (MT)

The MT method determines the electrical conductivity distribution of the sub-surface from measurements of natural transient electric and magnetic fields on the surface. The time variations of the earth´s electric and magnetic fields at the site are recorded simultaneously over a wide range of frequencies. The variations are analysed to obtain their spectra and apparent resistivities as a function of frequency.

The time-varying magnetic field *H* signal is the constant 'noise' present in the earth´s magnetic field. In the conducting earth, the changing magnetic field induces eddy currents and voltage, the latter being the electric signals, *E*. Current density in the earth depends on resistivity and, within a rock, the normal relationship between the electric field and the current density at each point is given by:

$$\boldsymbol{j} = \boldsymbol{E}/\rho \quad (9)$$

where $\boldsymbol{j}$ = Current density (A/m^2);
$\boldsymbol{E}$ = Electric field (mV/km);
ρ = Resistivity (Ωm).

The electric field is measured by monitoring the voltage difference between two electrodes at a distance l (m) apart:

$$V = l\,E \quad (10a)$$

In MT, the assumption is that *E* is constant over the length of the wire:

$$E = V/l \quad (10b)$$

The depth of penetration of the fields into the earth is inversely related to rock conductivity. In a uniform earth, *E* and *H* decrease exponentially with depth; the more conductive the earth is, the less is the penetration. The depth at which the fields have reduced to e^{-1} of their original value at the surface is called the skin depth:

$$\delta = \sqrt{2/\omega\mu\sigma} \quad (11a)$$

$$\approx 0.5\sqrt{\frac{\rho}{f}} \quad (11b)$$

where δ = Skin depth (km);
ω = Angular frequency, $\omega = 2\pi f$ (Hz);
μ = Permeability (H/m)

In a uniform or horizontally layered earth, all currents, electric fields, and magnetic fields are horizontal regardless of the direction from which these fields enter the earth. This is because of the high conductivity of the earth relative to the air (Vozoff, 1972). Furthermore, the currents and electric fields are at right angles to the associated magnetic fields at each point. The impedance tensor relates to the orthogonal components of the horizontal electric and magnetic fields:

$$\begin{pmatrix} E_x \\ E_y \end{pmatrix} = \begin{pmatrix} Z_{xx} & Z_{xy} \\ Z_{yx} & Z_{yy} \end{pmatrix} \begin{pmatrix} H_x \\ H_y \end{pmatrix} \; (\boldsymbol{E} = \boldsymbol{ZH}) \tag{12}$$

or

$$E_x = Z_{xx}H_x + Z_{xy}H_y \tag{13}$$

$$E_y = Z_{yx}H_x + Z_{yy}H_y \tag{14}$$

Each component of the impedance tensor, Z_{ij}, is composed of real and imaginary parts. They have both magnitude and phase.

For a 1D earth, conductivity varies only with depth and consequently the diagonal elements of the impedance tensors, Z_{xx} and Z_{yy} (which couple parallel electric and magnetic field components) equal zero, while the off-diagonal components (which couple orthogonal electric and magnetic field components) are equal in magnitude, but have opposite signs:

$$Z_{xx} = Z_{yy} = 0 \tag{15a}$$

$$Z_{xy} = -Z_{yx} \tag{15b}$$

For a homogeneous earth (1D), when electromagnetic plane waves propagate vertically downward, the ratio of the electric to the magnetic field intensity is a characteristic measurement of the electromagnetic properties of the medium (Keller and Frischknecht, 1966):

$$Z_{xy} = \frac{i\omega\mu_o}{k} = \frac{E_x}{H_y} \tag{16}$$

where Z_{xy} = Characteristic impedance;
ω = Angular frequency $(2\pi f)$, where f is frequency (Hz);
μ_0 = Magnetic permeability in vacuum (H/m);
$E_{x,y}$ = Electric field (V/m) in *x,y* direction;
$H_{x,y}$ = Magnetic intensity (A/m) in *x,y* direction;
$k = \sqrt{i\omega\mu_0(i\omega\varepsilon + \sigma)}$ is the wave propagation number;
ε = Dielectric permittivity (F/m);
σ = Electrical conductivity (S/m).

For the quasi-stationary approximation, $\sigma \gg \omega\varepsilon$, the wave propagation number is approximated by $k = \sqrt{i\omega\mu_0\sigma}$ and Equation 16 can be written as:

$$Z_{xy} = \frac{i\omega\mu_0}{\sqrt{i\omega\mu_0\sigma}} = \sqrt{i}\sqrt{\omega\mu_0\rho} = \sqrt{\omega\mu_0\rho} \times e^{\frac{i\pi}{4}} \tag{17}$$

Equation 17 shows that the phase difference between E_x and H_y is $\pi/4 = 45°$. For a homogeneous earth (1D), the resistivity is given as:

$$\rho_{xy} = \frac{1}{\omega\mu_0}\left|Z_{xy}\right|^2; \; \theta_{xy} = arg(Z_{xy}) \tag{18}$$

$$\rho_{yx} = \frac{1}{\omega\mu_0}\left|Z_{yx}\right|^2;\ \ \theta_{yx} = arg(Z_{yx}) \tag{19}$$

The apparent resistivity calculated from the off-diagonal elements of the impedance tensor for the 1D case like in Equations 18 and 19 should be the same. However, the earth is never 1D and the two resistivities in the *xy* direction and in the *yx* direction are different. By rotating the impedance tensor, we obtain different values for the resistivity. This presents a serious problem since we are never sure which value to use; *xy* or *yx*, as each gives different models.

The determinant of the impedance tensor was used for 1D inversion in this work, which is rotationally invariant (the resistivity value does not change with rotation); it is a kind of average value of the apparent resistivity. The determinant value is calculated as shown in Equation 20:

$$\rho_{det} = \frac{1}{\omega\mu_0}|Z_{det}|^2 = \frac{1}{\omega\mu_0}\left|\sqrt{Z_{xx}Z_{yy} - Z_{xy}Z_{yx}}\right|^2;\ \ \theta_{det} = \arg(Z_{det}) \tag{20}$$

For a 2D earth, it is assumed that the resistivity varies with depth and also in one lateral direction, and that the resistivity is constant in the other horizontal direction. The direction along which the resistivity is constant is called the electric strike. If the field setup coordinate system is not parallel and perpendicular to the electric strike, the MT impedance tensor data are mathematically rotated with one axis perpendicular to the electrical strike and the other axis parallel to it, through minimising the diagonal elements of the impedance tensor. Thereby, we get Z_{xx} and Z_{yy} close to zero, like in the 1D case, but the difference is that, in 2D, $Z_{xy} \neq -Z_{yx}$. Sometimes, it is not possible to find a strike direction that satisfies the condition: $Z_{xx} \approx Z_{yy} \approx 0$, this would be due to 3D subsurface resistivity structure.

4. TEM AND MT INSTRUMENTATION AND FIELD SET UP

The exploration geophysics Fellows participated in two days of field work in Eyjafjördur, North Iceland. It was aimed at introducing the participants to the TEM and MT equipment, field lay-out and data acquisition. To have a hands-on participation, the team joined the Iceland GeoSurvey technical staff that had been contracted by Nordurorka, the company that runs the Akureyri district heating system. The resistivity survey covered Botn/Hrafnagil and Grýta low-temperature geothermal fields with the target of siting additional exploration wells for the district heating system.

4.1 TEM instrumentation and field set-up

Instrumentation: The TEM instruments used were owned by Iceland GeoSurvey – ÍSOR, and consisted of Geonics PROTEM-67 including a digital receiver, transmitter, generator, transmitter loop (300 × 300) m and two sets of receiver loops, a circular loop of effective area 100 m^2 and a bigger loop of 5613 m^2 effective area.

Field procedure: The receiver and transmitter are turned on to warm up their crystal internal clocks for about 30 minutes before being synchronized. The square transmitter loop, 300 m × 300 m, is laid out with the aid of a triangular prism to achieve a square loop. The transmitter loop is connected to the transmitter by use of black and red banana jackets. The transmitter is connected to a generator and power module which amplifies the 60 VDC maximum output to approximately 160 VDC. With the transmitter loop connected to the transmitter, the motor generator is turned on and the output transmitter voltage is set to 110-120 VAC.

A number of settings are made in the receiver which includes: the repetition rates for which 20 gates were selected, 1D coil type, turn-off time recorded. Once the crystals have warmed-up, the transmitter and receiver are connected with a crystal synchronization cable and internal synchronization is

performed adjusting transmitter frequency to match receiver frequency. Two receiver loops with effective areas of 100 and 5613 m^2 and two transmitted current frequencies of 2.5 and 25 Hz were used. The receiver is connected to the receiver loop and gain, transmitted current and frequency are selected before the measurement is taken. The data can be viewed as a graph or values and various measurements can be done and stacked together at the same location. The data are stored in internal memory and downloaded onto a host computer via standard RS-232 ports.

4.2 The magnetotelluric field measurements

Instrumentation: For the magnetotelluric soundings, a total of three stations were deployed, two consisting of five components and one station with two components. This was done in addition to demobilising and preliminary data analysis of each station.

Five component data acquisition (MTU-5A) instruments manufactured by Phoenix Geophysics, Canada were used and consisted of the following: 5 electrodes, MTU-A acquisition unit, GPS antenna, 3 magnetic field induction coils and a 12 V DC battery.

Field procedure: The setup orientation was done by use of a compass. A typical five component MT unit comprised of an MTU data logger which is placed at the centre, oriented to the magnetic north for ease of reference and grounded. In the sounding, the two perpendicular horizontal components of the electric field (E_x, E_y) are measured through the use of a couple of pairs of electrodes; for the magnetic field measurements, 3 induction coils are involved, 2 of which measure 2-horizontal perpendicular components (H_x, H_y) and 1 coil measures the vertical component (H_z) as illustrated in Figure 5. Precaution against cultural noise was adequately considered and this involved siting the stations away from trees, power lines, buildings, traffic, turning-off electric fences and burying magnetic coils to a depth of at least 0.3 m in addition to levelling them horizontally by use of a spirit level.

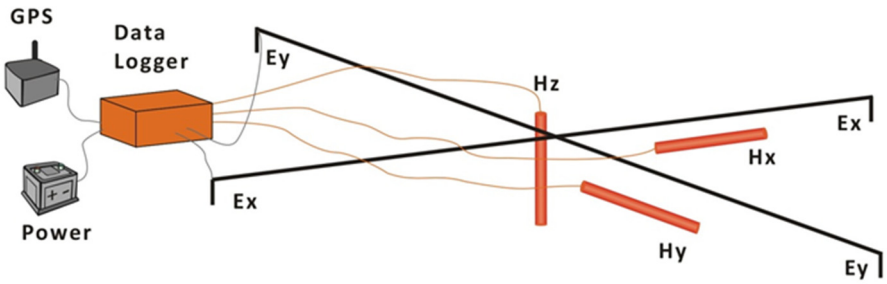

FIGURE 5: The setup of a magnetotelluric sounding (modified from Flóvenz et al., 2012)

5. CHARACTERISTICS OF THE THEISTAREYKIR HIGH-TEMPERATURE AREA

The Theistareykir high-temperature geothermal area lies in the Theistareykir fissure swarm within the volcanic zone in northeast Iceland (Figure 6). For centuries it hosted the main sulphur mine in Iceland, providing the Danish king with raw material for gun powder (Ármannsson et al., 1986). The active part of the geothermal area lies in the eastern half of the Theistareykir fissure swarm. The geothermal activity covers an area of 10.5 km^2. The most intense activity is on the northwest and northern slopes of Mt. Baejarfjall and in the pastures extending from there northwards to the western part of Mt. Ketilfjall.

Hydrothermal alteration is evident on the western side of the swarm, but surface thermal activity seems to have died out some 1,000 years ago. If the old alteration in the western part of the swarm is considered to be a part of the thermal area, its coverage is nearly 20 km^2 (Grönvold and Karlsdóttir, 1975).

Saemundsson (2007) thoroughly studied the geology of Theistareykir area (Figure 7) and the following description is based on his publication. The bedrock in the area is divided into hyaloclastite ridges formed by subglacial eruptions during the ice age, interglacial lava flows, and recent lava flows (younger than 10,000 years), all basaltic. Acidic rocks are found on the western side of the fissure swarm, from subglacial eruptions up to the last glacial period. Rifting is still active in the fissure swarm.

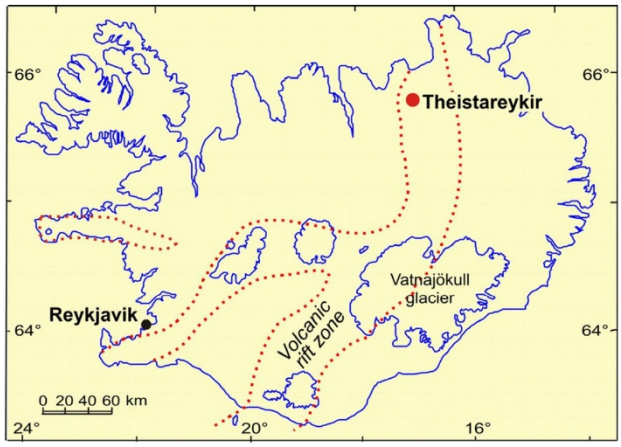

FIGURE 6: Map showing location of Theistareykir high-temperature geothermal field

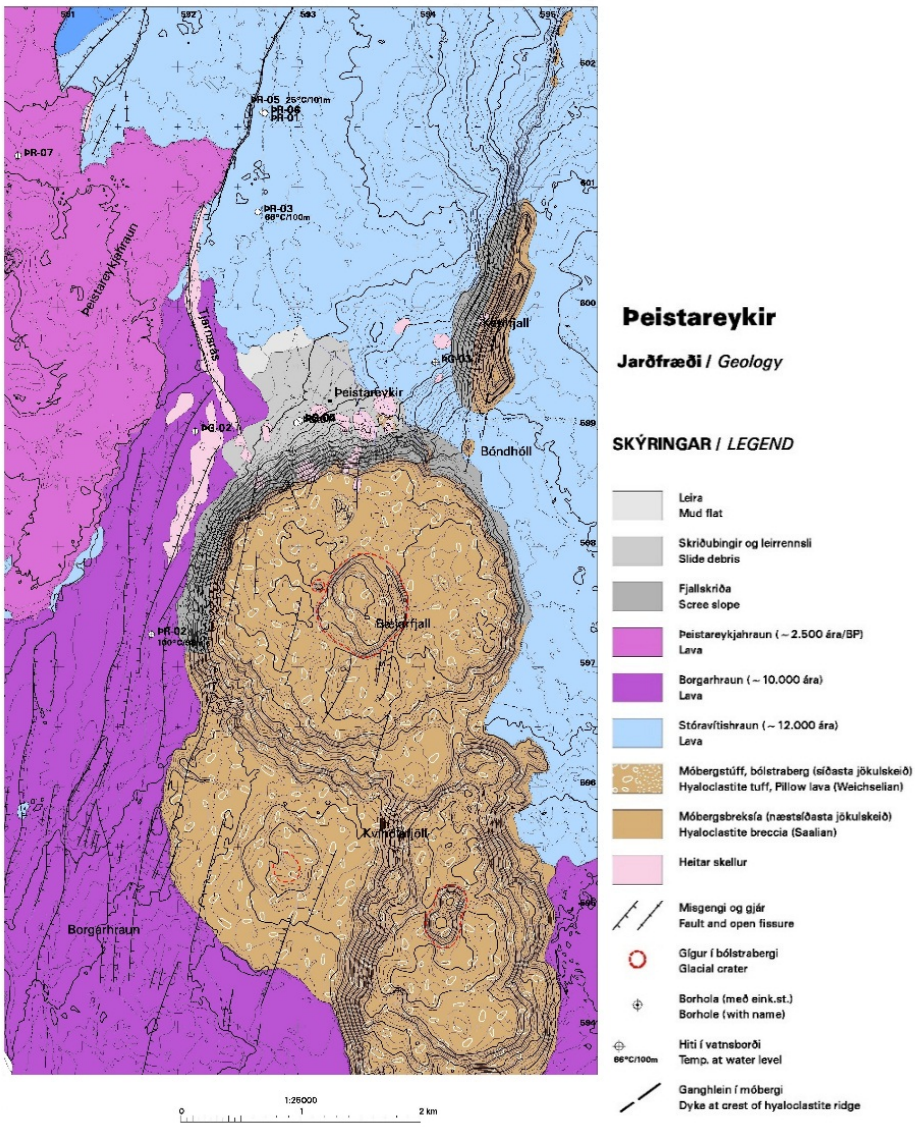

FIGURE 7: Geological map of Theistareykir geothermal area (modif. from Saemundsson, 2007)

Volcanic activity has been relatively dormant in the area in recent times with approximately 14 eruptions in the last 10,000 years but none in the last 2,500 years. Large earthquakes up to a magnitude of 6.9 occur mainly north of the area in the Tjörnes fracture zone, which is a right-lateral transform fault in the fissure swarm. The Tjörnes fracture zone strikes northwest, crosscutting the north striking fractures as it enters into the fissure swarm north of the thermal area. The volcanic activity ceases in the fissure swarm as it crosses the Tjörnes fracture zone although its northern part remains seismically active (Ármannsson et al., 1986). The most active parts of the area are related to active fractures, increasing permeability and acting as conduits for geothermal fluids to flow.

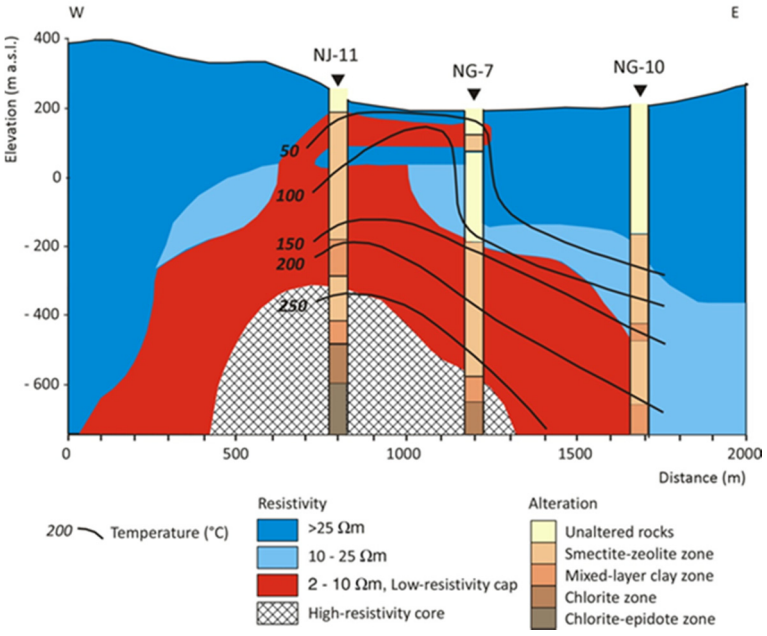

FIGURE 8: Resistivity cross-section from the Nesjavellir geothermal field, SW-Iceland, showing also alteration zoning and temperature (Árnason et al., 1987b)

Árnason et al. (1987a; 2000) and Flóvenz (2012) discussed the resistivity structure of Icelandic high-temperature geothermal systems delineated by using electric and electromagnetic methods. As partly discussed in Section 3.1, resistivity is controlled by hydrothermally altered minerals, which are linked with the temperature distribution in the reservoir. At 100-220°C, alteration zones are dominated by smectite-zeolite minerals, while at temperatures of 220-240°C, the zeolites disappear and smectite is replaced by chlorite. At temperatures exceeding 250°C, chlorite and epidote are the dominant alteration minerals (Figure 8). The electrical conductivity is explained by the presence of loosely bound electrons and a layered clay silicate with the high cation exchange capacity structure of hydrated smectite, while in chlorite the cations have a fixed crystal lattice. Because the mineral alteration is dependent on temperature, the resistivity reflects a thermometer in high-temperature geothermal reservoirs, that is, if the alteration is in equilibrium with the temperature. Sometimes an area has cooled down, or part of an area, and there the resistivity reflects a maximum thermometer. The relationship between resistivity, hydrothermal alteration and temperature from the high-temperature geothermal field Nesjavellir is shown in Figure 8. Alteration minerals can also indicate lower temperatures than those measured in the wells. This has been interpreted as indicating a young system still heating up with alteration lagging behind and, therefore, not in thermal equilibrium.

Between 2004 and 2006, a resistivity survey was conducted in the Theistareykir geothermal area using the TEM method with a depth penetration of 800-1000 m. The results were presented by Karlsdóttir et al. (2006). A high-resistivity core below a low-resistivity layer, indicating a high-temperature geothermal resource, was confirmed at depths as shallow as 200 m. Results of the clay analysis from borehole ThG-1 showed a good correlation between alteration, resistivity and temperature. The results of the clay analysis from ThG-2 showed a good correlation between resistivity and alteration, although there were a number of alteration minerals that would indicate cooling at the top of the system. This was backed up by temperature measurements.

Exploration drilling started in 2002 with the completion of well ThG-1, a vertical well reaching 1953 m below the surface. Comparing results of a sample analysis from well ThG-1 (Gudmundsson et al., 2002) with the resistivity measurements near the well showed that smectite is dominant down to 200 m. Below

230 m, there is a mixed smectite-chlorite layer with chlorite being dominant. Similarly, very low resistivity values, 2-3 Ωm, are seen down to 200 m; thereafter, the resistivity becomes considerably higher. This indicates that there is considerable correlation between resistivity and subsurface alteration.

6. RESISTIVITY PROSPECTING OF THE THEISTAREYKIR GEOTHERMAL FIELD

Iceland GeoSurvey - ÍSOR carried out TEM and MT soundings in the Theistareykir geothermal field between 2009 and 2011. From that survey, two profiles (profiles 3 and 4) with nine and seven TEM and MT soundings, respectively, were processed and interpreted as a part of this project. For location, see Figure 9.

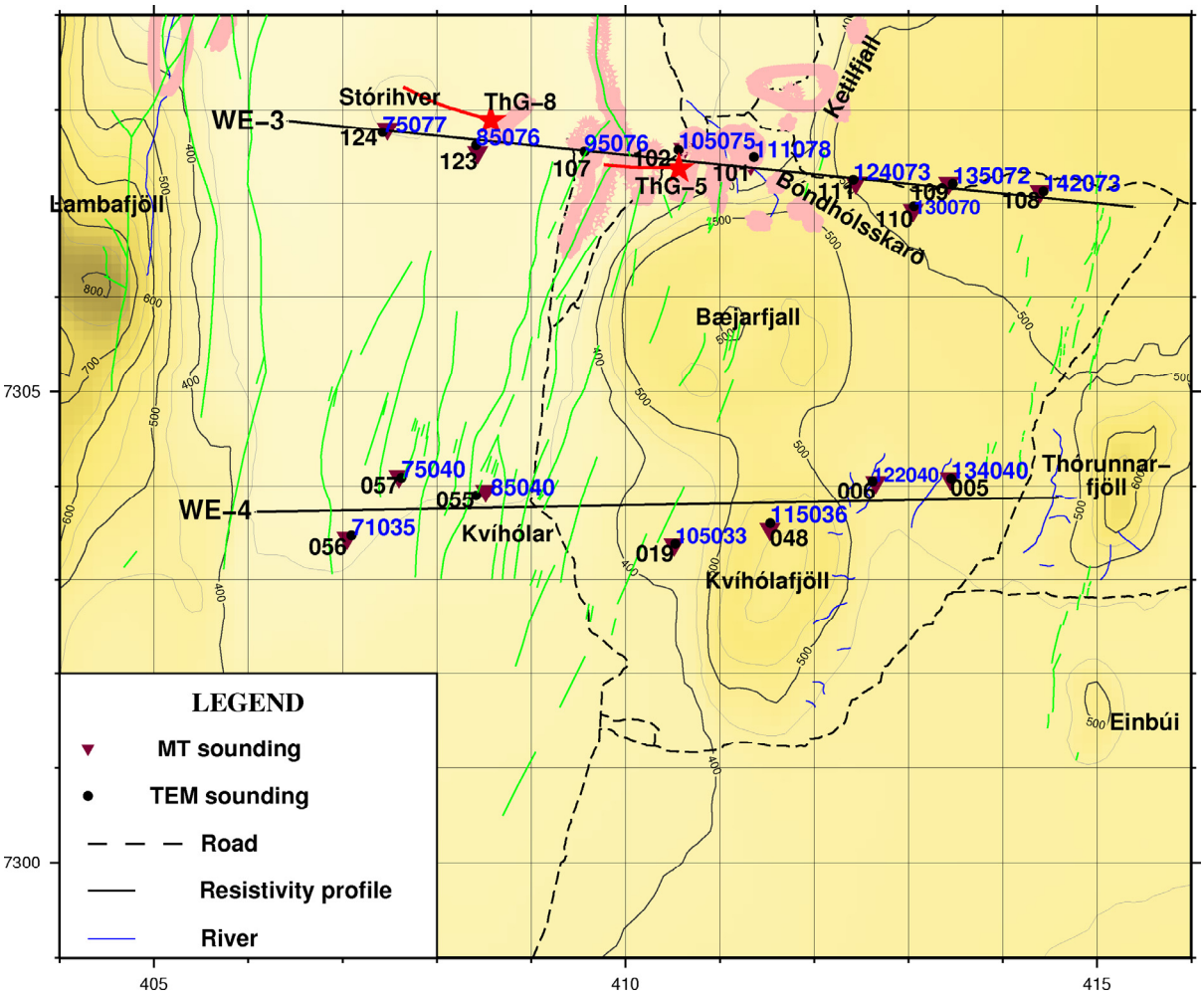

FIGURE 9: Location of the resistivity profiles and TEM and MT soundings; red (dark) stars denote directional wells (ThG-5 and ThG-8) and green (grey) lines geological fractures. Surface manifestations are light red (grey) shades

6.1 TEM data processing and inversion

The TemX program written by Árnason (2006a) at ÍSOR was used to read the raw files from the PROTEM receiver. The TemX program performs normalisation of the voltages with respect to the transmitted current, turn off time, gain and effective area of the receiver and transmitter coils and then

displays all the data graphically, allowing the user to omit outliers; it also calculates averages over datasets and calculates late time apparent resistivity (Árnason, 2006a).

For the inversion of TEM data, the TEMTD program (Árnason, 2006b) was used to perform the 1D Occam inversion of the data shown in Appendix I (Kahwa, 2012). The program assumes a square source loop and the receiver loop/coil at the centre of the source loop. The current wave-form is assumed to be a half-duty bipolar semi-square wave with exponential current turn-on and linear current turn-off.

The program offers the possibility of keeping models smooth, both with respect to resistivity variations between layers and layer thicknesses. The damping can be done both on the 'first derivatives', which counteracts sharp steps in the model (on log scale), and on 'second derivatives' which counteracts oscillations in the model values (on log scale). The actual function that is minimised is, in this case, not just the weighted root-mean-square mistfit, chsq, but the 'potential':

$$Pot = Chisq + \alpha \times DSI + \beta \times DS2 + \gamma \times DD1 + \delta \times DD2 \qquad (21)$$

where *DS1* and *DS2* are the first and second derivatives of log-conductivities in the layered model and *DD1* and *DD2* are the first and second order derivatives of the algorithms of the ratios of layer depths. The coefficients α, β, γ and δ are the relative contributions of the different damping terms and are specified by the user.

In the minimum structure (Occam) inversion, the layers' thicknesses are kept fixed, equally spaced on log scale, and the conductivity distribution is forced to be smooth by adjusting α and β in Equation 21. Typical Occam inversion models of TEM soundings are shown in Figure 10.

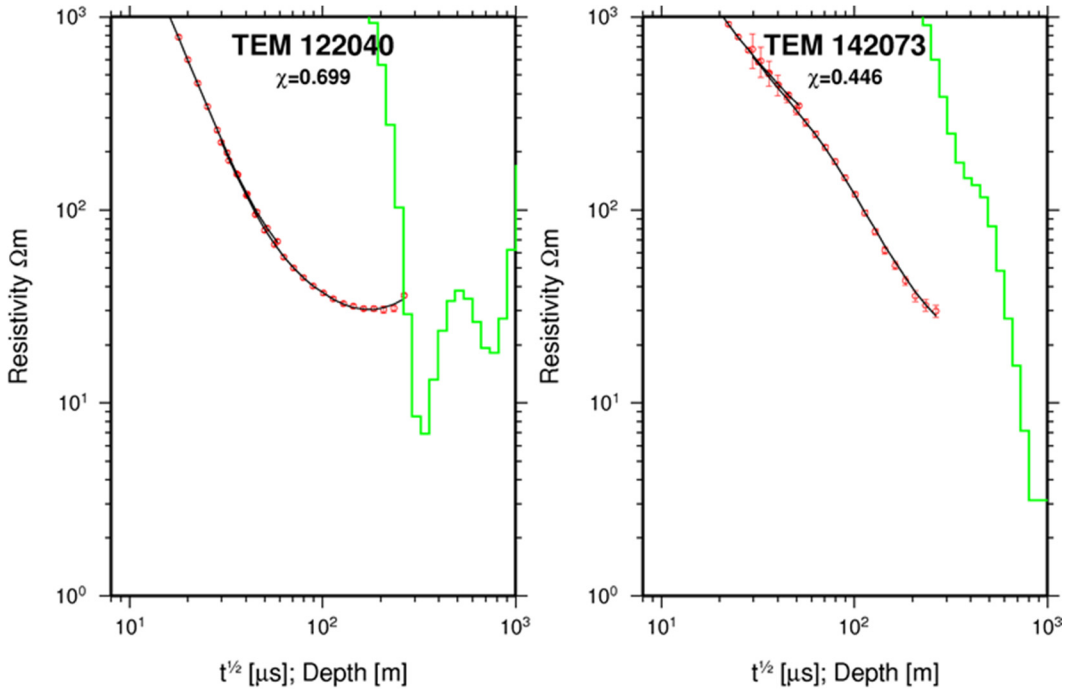

FIGURE 10: Typical TEM soundings from Theistareykir area and 1D inversion models. Red (dark) circles: measured late-time apparent resistivities; black line: apparent resistivity calculated from the model shown in green (grey). The numbers on the top of the figures (TEM 122040 and 142073) correspond to the names of the stations; χ shows the fit between measured and calculated data

6.1.1 TEM resistivity cross-sections

From the 1D inversion results of the TEM data, cross-sections were plotted using the program TEMCROSS (Eysteinsson, 1998) developed at Iceland GeoSurvey. The program calculates the best

line between selected sites on the profile and plots resistivity isolines based on the 1D models generated for the soundings. The program contours the logarithm of the resistivity; an exponential colour scale through contour number lines gives resistivity values. A number of cross-sections at varying depth were plotted for the two profiles, depending on the structures of interest and the extent of depth penetration of the MT sounding.

Profile WE_3 lies to the south of Stórihver, across Theistareykir and Bóndhólsskard, cutting through wells ThG-5 and ThG-8 (location shown in Figure 9). TEM data were used to plot a cross-section for the uppermost 600 m a.s.l. (Figure 11). To the east and west of Bóndhólsskard, a high-resistivity layer (>100 Ωm) is seen down to a depth of 120 m to the west and over 400 m to the east. This high resistivity reflects an unaltered rock formation. Below the high-resistivity layer, a low-resistivity layer is found that reaches the surface in Theistareykir where widespread surface manifestations are seen (Figure 9). This low-resistivity layer correlates with the smectite-zeolite alteration zone. Below this low-resistivity cap rock there emerges a high-resistive core (>100 Ωm) correlating with the chlorite-epidote alteration zone.

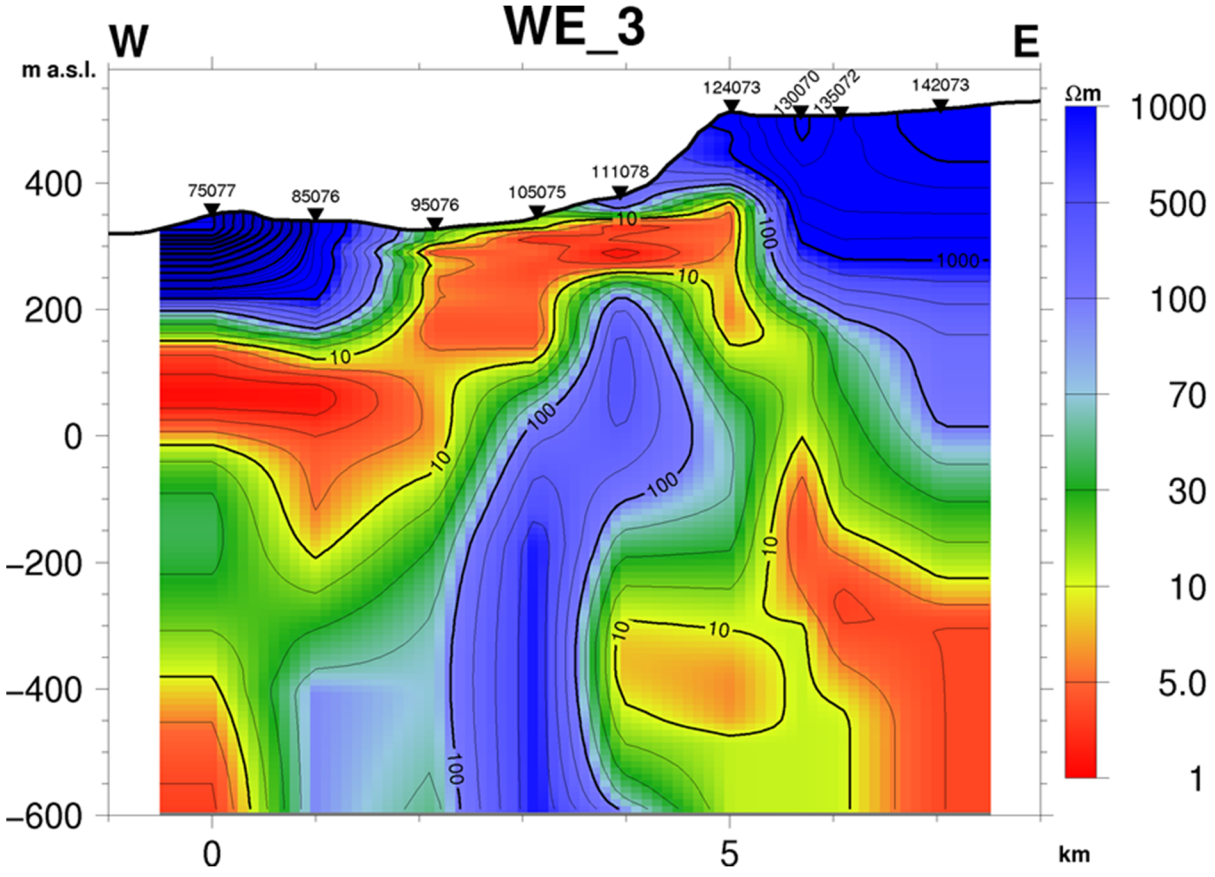

FIGURE 11: Resistivity profile WE_3 based on TEM data, reaching down to 600 m b.s.l.

Profile WE_4 lies to the north of Kvíhólar and Kvíhólafjöll all the way east to Thórunnarfjöll (location shown in Figure 9). It presents a typical resistivity section expected in a high-temperature geothermal area with a high-resistive layer of unaltered rock formation close to the surface down to a depth of 200-250 m below the surface (Figure 12). At 0-200 m a.s.l., the low-resistivity layer emerges shallower to the east than to the west, extending to a depth of 100 m b.s.l. to the east and significantly deeper to the west. Below the conductive layer there is a resistive core (> 100 Ωm) which correlates with the chlorite-epidote high-temperature hydrothermal alteration zone.

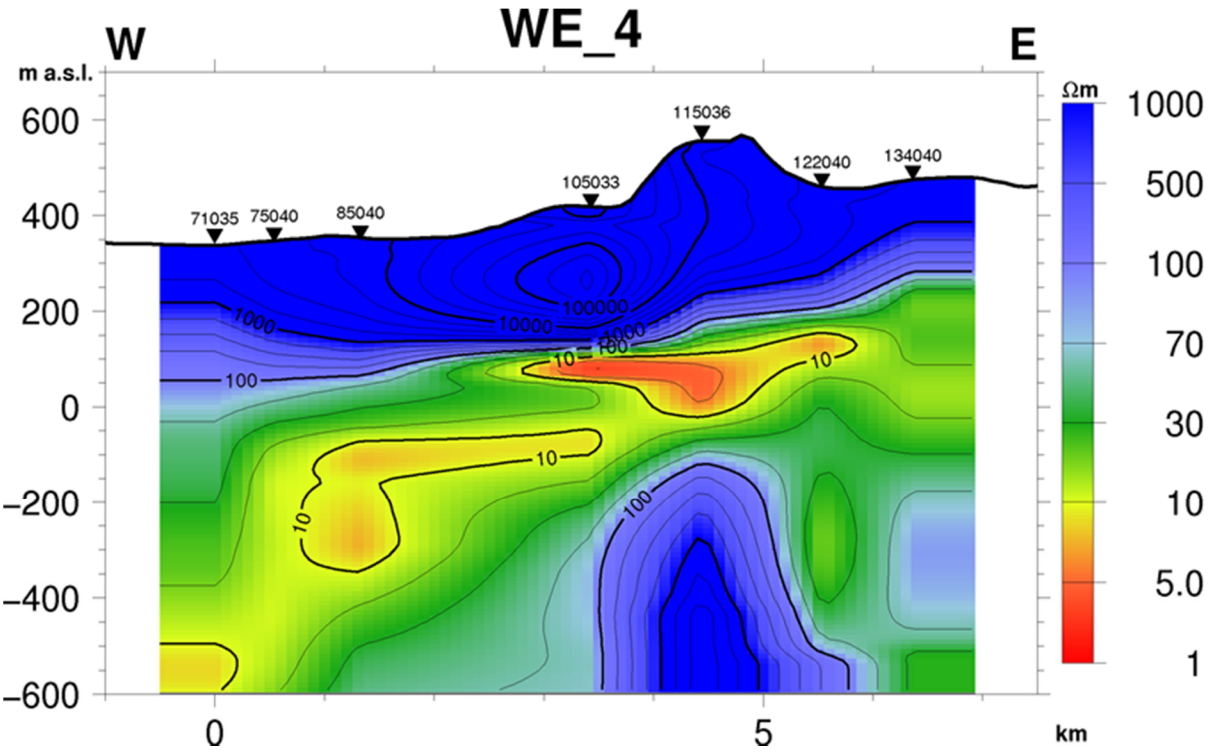

FIGURE 12: Resistivity profile WE_4 based on TEM data, reaching down to 600 m b.s.l.

6.1.2 TEM iso-resistivity maps

The TEMRESD program (Eysteinsson, 1998) was used to generate iso-resistivity maps from the 1D Occam models. The resistivity is contoured and coloured in logarithmic scale. Theistareykir area is on average 280-550 m a.s.l. For this work, iso-resistivity maps are presented from 300 m a.s.l. down to 10,000 m b.s.l. with the upper iso-resistivity maps reflecting the TEM resistivity structures while deeper structures are reflected from the MT data.

A resistivity map at 300 m a.s.l. from TEM data is shown in Figure 13. In the central part of the plot, a low-resistivity anomaly trending in an E-W

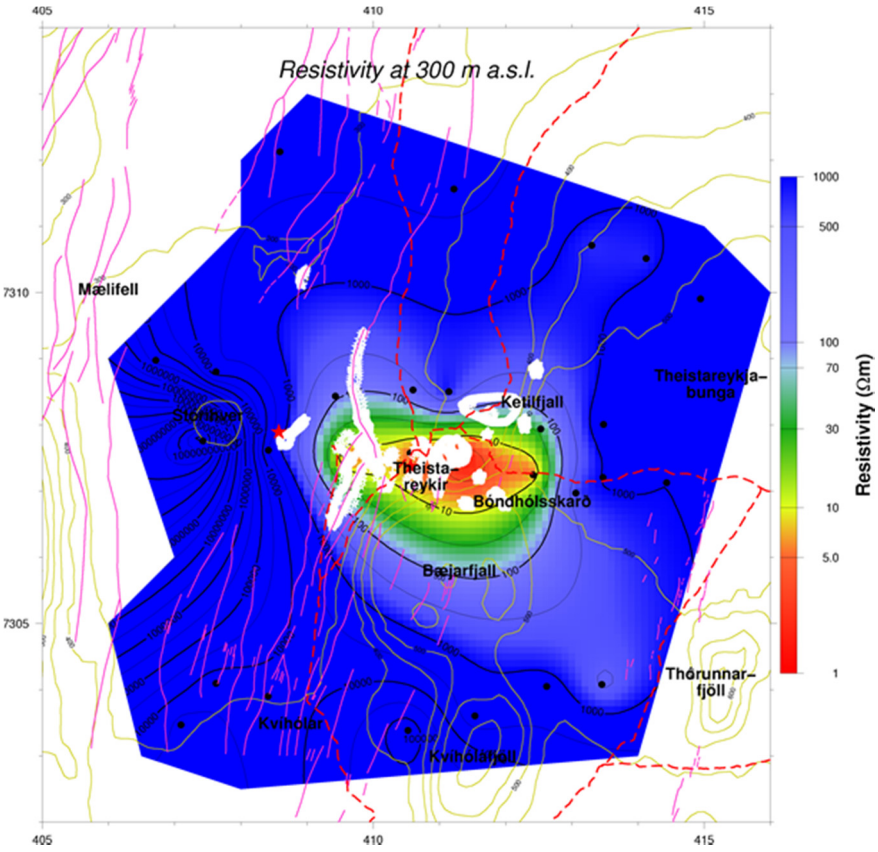

FIGURE 13: Resistivity in the Theistareykir area based on TEM data at 300 m a.s.l. Black dots are MT soundings, red (dark) lines are geological fractures, white shades are surface manifestations, magenta (dark) stars are wells and red (dark) dashed lines are roads

direction and reaching to the surface is observed. This is due to the smectite-zeolite alteration layer that reaches the surface and is evident by the numerous surface alterations in the area (Figure 9). The low-resistivity body is surrounded by the high-resistivity un-altered rock formation. The low-resistivity cap reaching the surface is the up-flow region during the formation of the geothermal system which may have cooled in some areas due to scaling in fluid conduits or fractures which are the passages for hydrothermal fluids to the surface.

6.2 MT data processing and inversion

The time series files from the MT equipment were processed using the program SSMT2000 provided by Phoenix Geophysics in Canada. The site parameters, including site name, dipole length, setup orientation and coil numbers were verified in the TBL file before verifying acquisition times to check on how long the stations and remote station were deployed. Calibration files were inserted. The time series were then Fourier transformed into the frequency domain and the cross- and auto-powers were calculated using the robust processing method; for stations without a remote reference station, local H was used for processing and producing the apparent resistivity and phase curves as a function of frequency. The resistivity and phase were then graphically edited by the MTEditor program to remove the noisy data points and evaluate smooth curves for both phase and apparent resistivity. The final cross- and auto powers, as well as relevant MT parameters, were calculated from them: impedances, apparent resistivity and phase, coherencies, and strike directions were stored in .edi format and used as inputs to the TEMTD program for joint inversion (Figure 14).

Figure 14 shows the following in the upper half:

a) Apparent resistivity for both main modes (ρ_{xy} and ρ_{yx}) was calculated in the measured directions i.e. *x,* the magnetic north, and *y,* magnetic east. Black circles denote the apparent resistivity derived from the rotationally invariant determinant of the impedance tensor (see Equation 20).

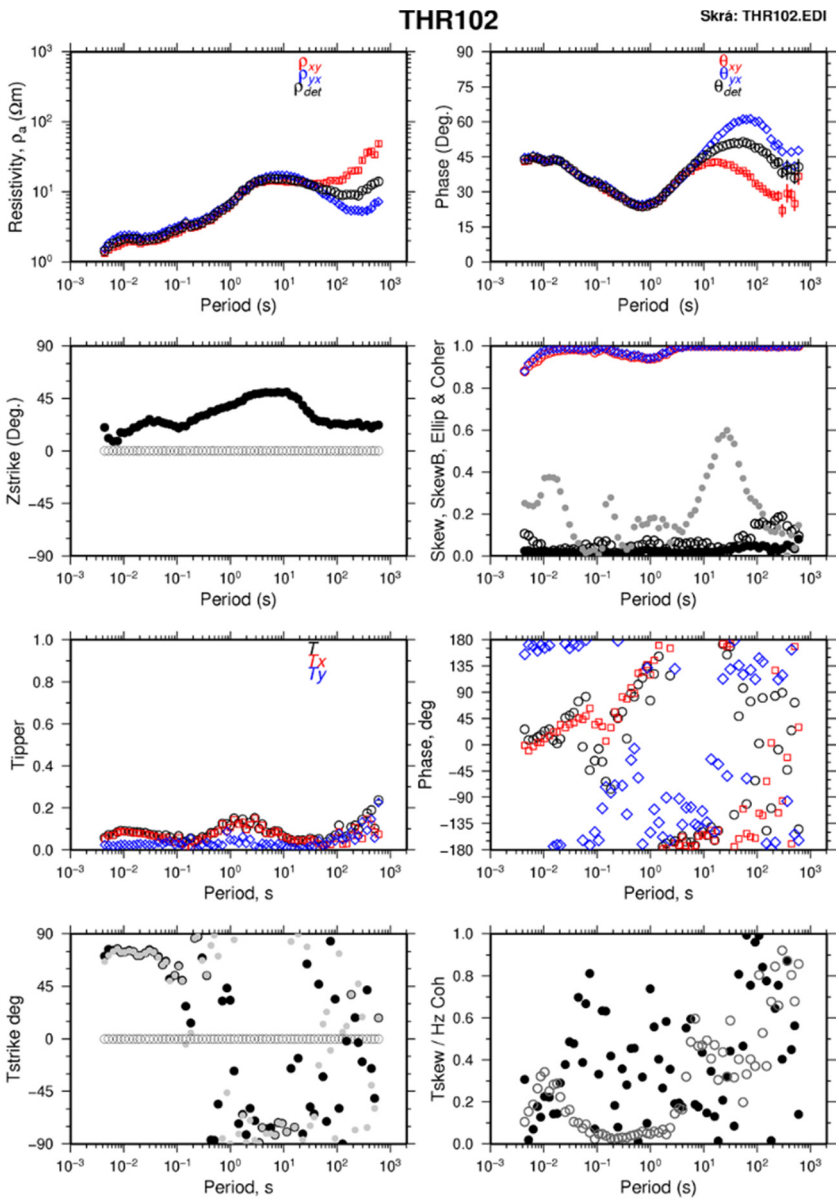

FIGURE 14: Results of MT data processing

b) Apparent phase (θ_{xy} and θ_{yx}) was calculated in the measured directions. Black circles denote the apparent phase derived from the rotationally invariant determinant of impedance tensor.

c) Zstrike or the Swift angle gives the electrical strike (the horizontal rotation which maximises $\left(|Z_{xy}|^2 + |Z_{yx}|^2\right)$ for each frequency and is shown by filled circles. The direction used for calculating the apparent resistivity and phase is shown by unfilled circles. For two-dimensional electrical structures, a constant value of electrical strike was observed.

d) Three-dimensional indicators:

$Skew = \frac{|Z_{xx}+Z_{yy}|}{|Z_{xy}-Z_{yx}|}$

Swift skew is shown by filled circles. It is rotationally invariant and should be zero for 1D and 2D earth.

$SkewB = \frac{\sqrt{|Im(Z_{xy}Z_{yy}^{*}+Z_{xx}Z_{yx}^{*}|}}{|Z_{xy}-Z_{yx}|}$ or Bahr skew.

It is shown by unfilled circles. It is rotationally invariant and should be close to zero for both 1D and 2D earth.

$Ellip = \left|\frac{Z'_{xx}-Z'_{yy}}{Z'_{xy}+Z'_{yx}}\right|$ or ellipticity

It is shown by grey circles. It is calculated in the principle rotational coordinates and gives the axis rotation of the electrical field ellipse. A value of zero for both skew and ellipticity is a necessary and sufficient condition for two-dimensionality of the data.

Red (dark) and blue (grey) colours on the *skew*, *skewB*, *Ellip*, and *Coher* graph show the multiple coherencies of the electrical fields with respect to the horizontal magnetic fields in the measuring directions.

The results of the data processing of the 16 MT soundings are given in Appendix II in a special report including the appendices to this report (Kahwa, 2012).

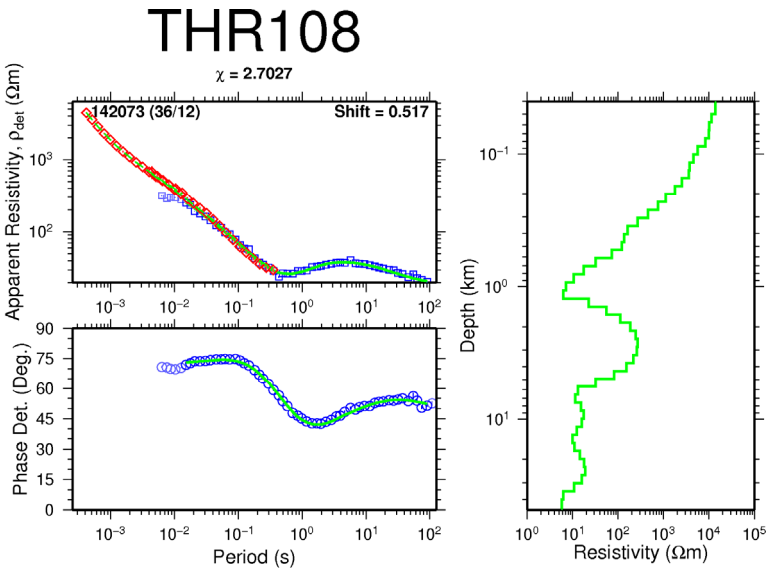

FIGURE 15: Typical result of a joint 1D inversion of TEM and MT soundings; red (dark) diamonds are measured TEM apparent resistivities and blue (grey) squares are the MT apparent resistivities. Solid lines show the response of the resistivity model to the right (green/grey). The shift multiplier is shown in the upper right hand corner of the apparent resistivity panel and the Chi square, χ, is the misfit

TEMTD was also used for joint inversion of TEM and MT data where the so-called static shift multiplier was determined. An example is given in Figure 15. The program uses a gnuplot graphics program for graphical display during the inversion process. The apparent resistivity and phases derived from the determinant of the MT tensor were inverted jointly with the nearby TEM data. The measured TEM apparent resistivity (red/ dark diamonds) curve that overlaps the MT apparent resistivity curve (blue) was used to correct the static shift; the shift multiplier of 0.517 is shown on the upper right corner (Figure 15). Results of joint 1D inversion of TEM and MT soundings and models are in Appendix III (Kahwa, 2012).

6.3 Static shift

The MT method, and all other resistivity methods that are based on measuring the electric field at ground surface, suffer from the static shift problem (Árnason et al., 2010).This phenomenon is caused by near-surface resistivity inhomogeneities close to the electric dipoles. Several methods have been advanced as possible solutions for the static shift problem in MT. DeGroot-Hedlin (1991) and Ogawa and Ushida (1996) proposed the use of an inversion algorithm on MT data to correct for static shift; this assumes that the static multipliers are random, and that the product of the shift multipliers for many soundings is close to one, which may not necessarily be correct.

The second and most reliable theory is to use the Central loop-induction TEM soundings to correct for static shift by jointly inverting both TEM and MT data. It is based on the fact that for TEM measurements at late times, there are no distortions due to near surface inhomogeneities since they do not measure the electric field. This has been tested by model calculations (e.g. Sternberg et al., 1988) and shown to be useful in correcting for static shifts.

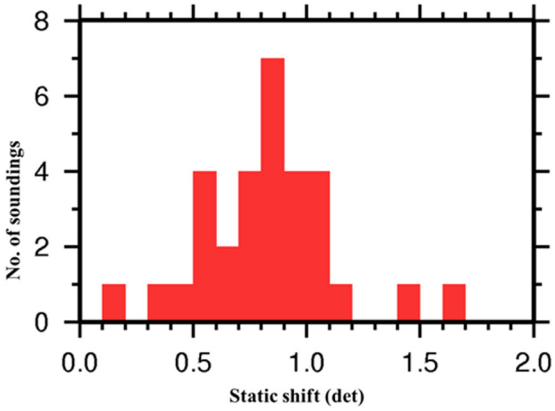

FIGURE 16: Histogram showing the values of static shift multipliers for the determinant apparent resistivity

Static shift analysis of 31 MT soundings was done using the TEMTD joint inversion code for MT and TEM soundings on profiles 3 and 4 with additional results from my UNU Fellow, Suriyaarachchi (2012), and then inverting for the rotational invariant determinant apparent resistivity and phase data. The shift factors are in the range of 0.2-1.7 while most MT determinant apparent resistivity curves were shifted down a factor of 0.9 (Figure 16). Figure 17 shows the spatial distribution of shift multipliers in Theistareykir area. However, there is no systematic correlation of shift multipliers with the station locations and thus one needs to apply the correction independent of other stations using the closest TEM sounding (200-500 m).

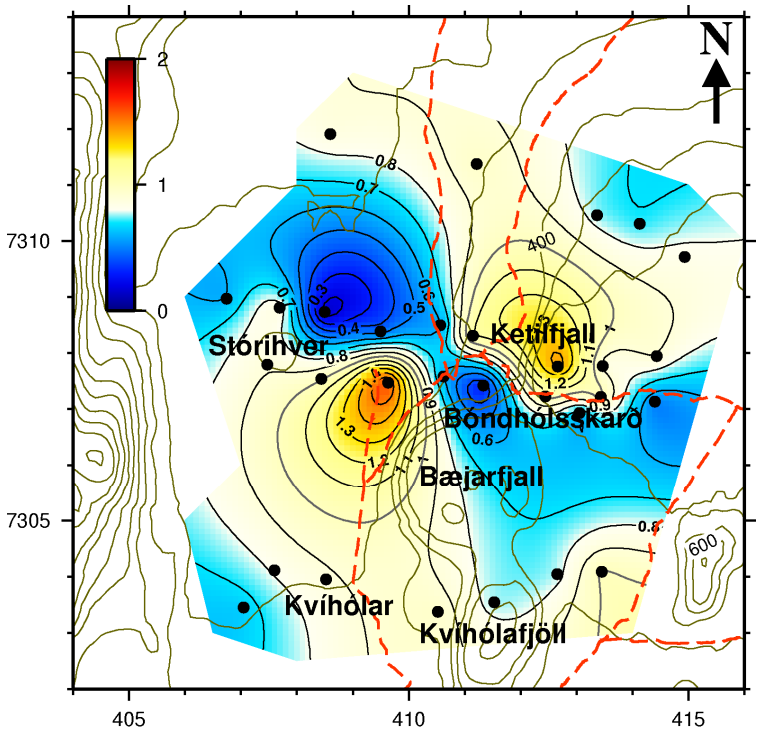

FIGURE 17: Spatial distribution of the static shift multipliers in Theistareykir geothermal area. Black dots are MT soundings and red/dark dashed lines are roads

6.4 Strike analyses and induction arrows

Strike directions are found by making directional analysis of MT data. Zstrike gives the electrical strike. It is the horizontal rotation which maximises the off-diagonal elements of the MT tensor (Z_{xy} and Z_{yx}) and minimises the diagonal ones (Z_{xx} and Z_{yy}), using the sum of the squared modules of these components (Teklesenbet, 2012). For periods 0.01-1 s, the main electric strike is found to be N-S for most of the MT sites (Figure 18) which is parallel to

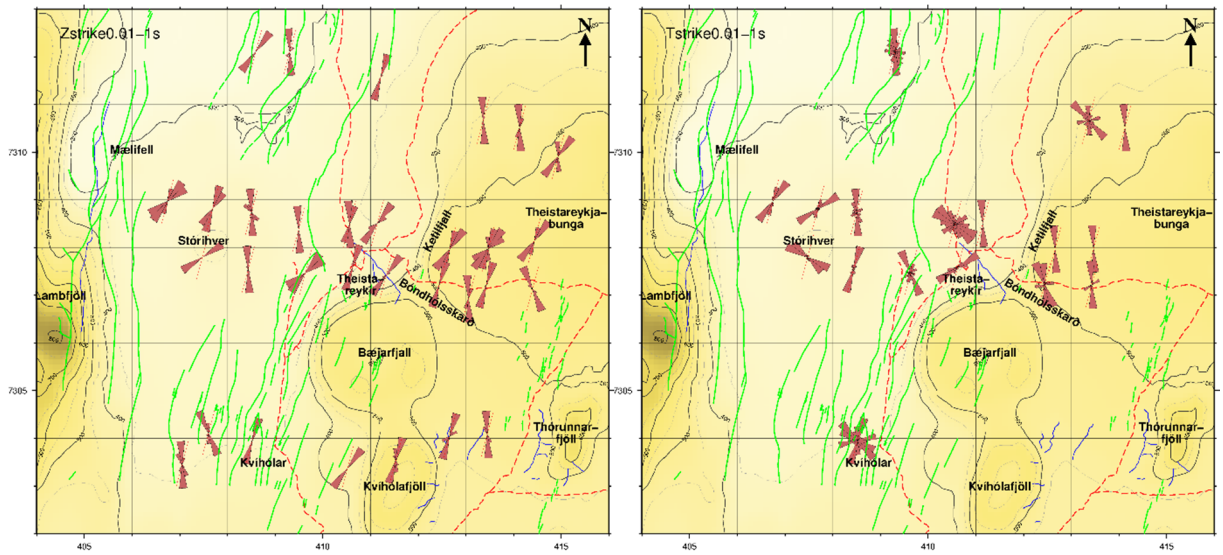

FIGURE 18: Rose diagram of the electrical strike based on a) Zstrike, and b) Tstrike for the period 0.01-1 s; green (grey) lines denote fractures and red (dark) dashed lines are roads

the Theistareykir fissure swarm, as can be observed from the geology of the area (Figure 7).

The Zstrike has 90° ambiguity and the strike direction cannot be determined using MT impedance data alone. This ambiguity can be resolved by using information from the Tipper vector if the vertical magnetic field (H_z) is available. Additional information such as local geology might help overcome this ambiguity. For Theistareykir area, many MT soundings lacked the H_z component and thus the Tipper strike was only calculated for the few soundings where the H_z component existed. From the Tstrike rose diagram for the period 0.01-1 s, it can be seen that the electric strike concurs with the N-S direction of Zstrike (Figure 18).

The magnetic transfer function or Tipper is a response which relates the vertical component of the magnetic field to the two horizontal components (Vozoff, 1991). This response is often displayed graphically in the form of induction arrows. Since vertical magnetic fields are generated by lateral conductivity gradients, induction arrows can be used to infer the presence or absence of lateral conductivity variations (Teklesenbet, 2012). These vectors, as they are independent of the MT impedance tensor, can provide valuable constraints on the dimensionality and strike analysis of the data.

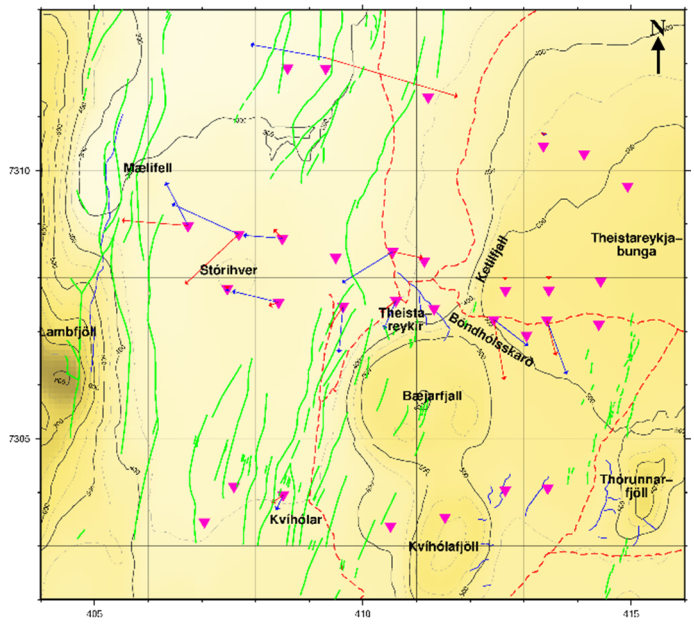

FIGURE 19: Induction arrows for Theistareykir area for the period 10 s (where H_z exists), real part (blue/grey) and imaginary part (red/dark)

Figure 19 shows the real part (blue/grey) and imaginary part (red/dark) of the arrows for a period of 10 seconds (corresponding to approximately 5 km depth considering a period of 10 s and resistivity of 10 Ωm) for soundings where the vertical magnetic component (H_z) was measured. The figure shows arrows pointing away from the conductor below Bóndhólsskard and close to Stórihver.

6.5 MT resistivity cross-sections

Cross-section WE_3 from joint inversion of TEM and MT data is shown in Figures 20 and 21. The cross-section in Figure 20 is plotted down to 5,000 m b.s.l. and clearly reveals the low-resistivity cap at shallow depth and the underlying the high-resistivity core (> 100 Ωm). The resistive core stretches from 1,000 m b.s.l. down to 4,000 m b.s.l. and correlates with the chlorite-epidote alteration zone. Below the resistive core there is a relatively conductive layer, seen better in Figure 21, which reaches down to 15.000 m b.s.l. This may indicate the heat source for the geothermal field.

Cross-section WE_4 from joint inversion of TEM and MT data is shown in Figure 22, reaching down to 2000 m b.s.l. Three layers are revealed by cross-section WE_4 and include a high-resistivity layer near the surface, due to un-altered formations; underlying it is a low-resistivity layer correlating to the smectite-zeolite alteration zone; and then the high-resistivity core, which emerges shallower to the east than the west.

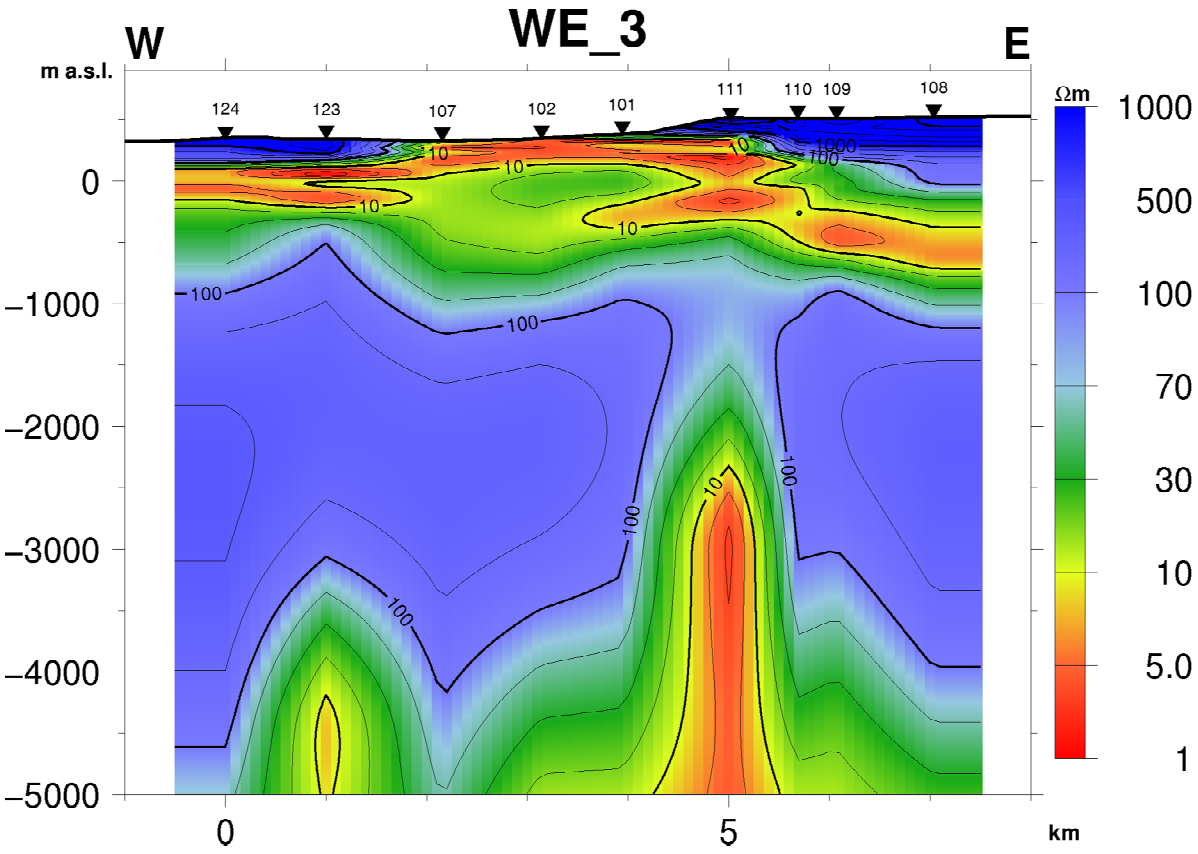

FIGURE 20: Resistivity profile WE_3 based on 1D joint inversion of TEM and MT data, reaching down to 5,000 m b.s.l.

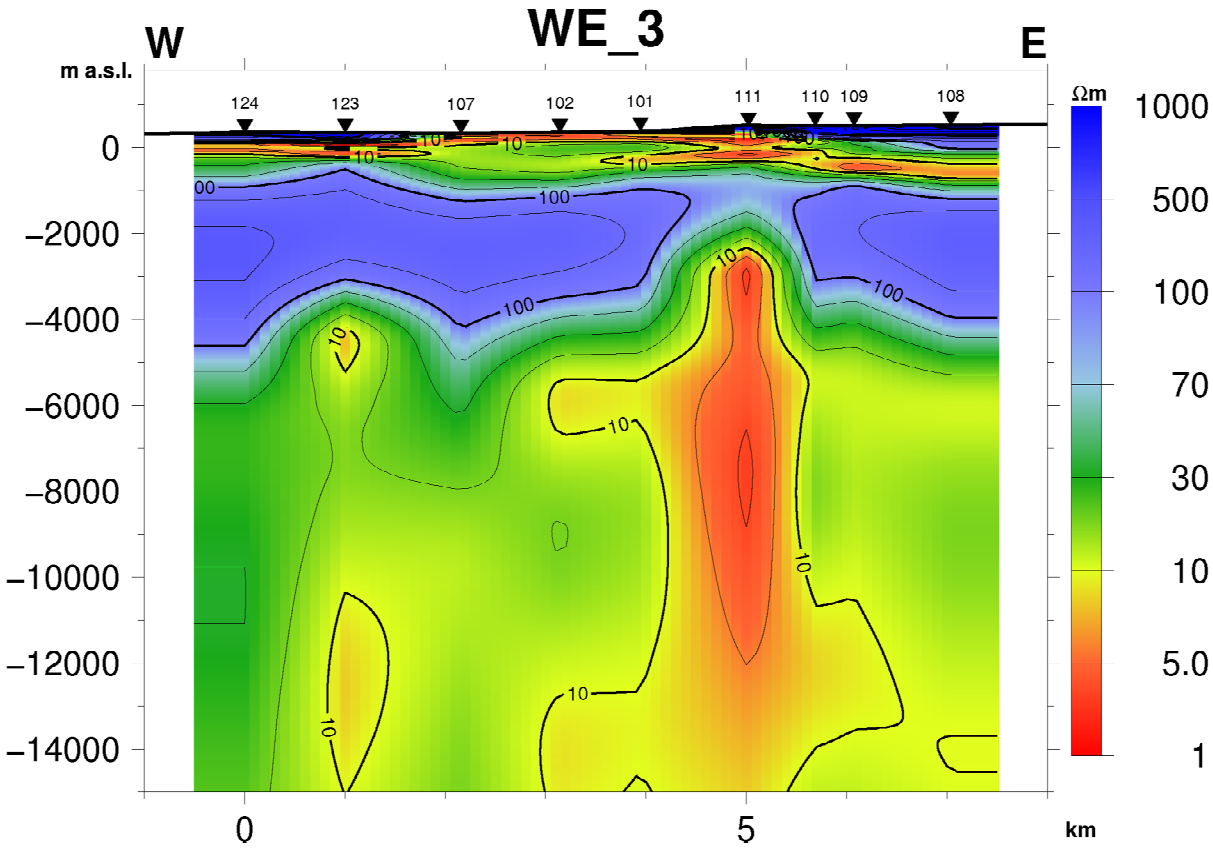

FIGURE 21: Resistivity profile WE_3 based on 1D joint inversion of TEM and MT data, reaching down to 15,000 m b.s.l.

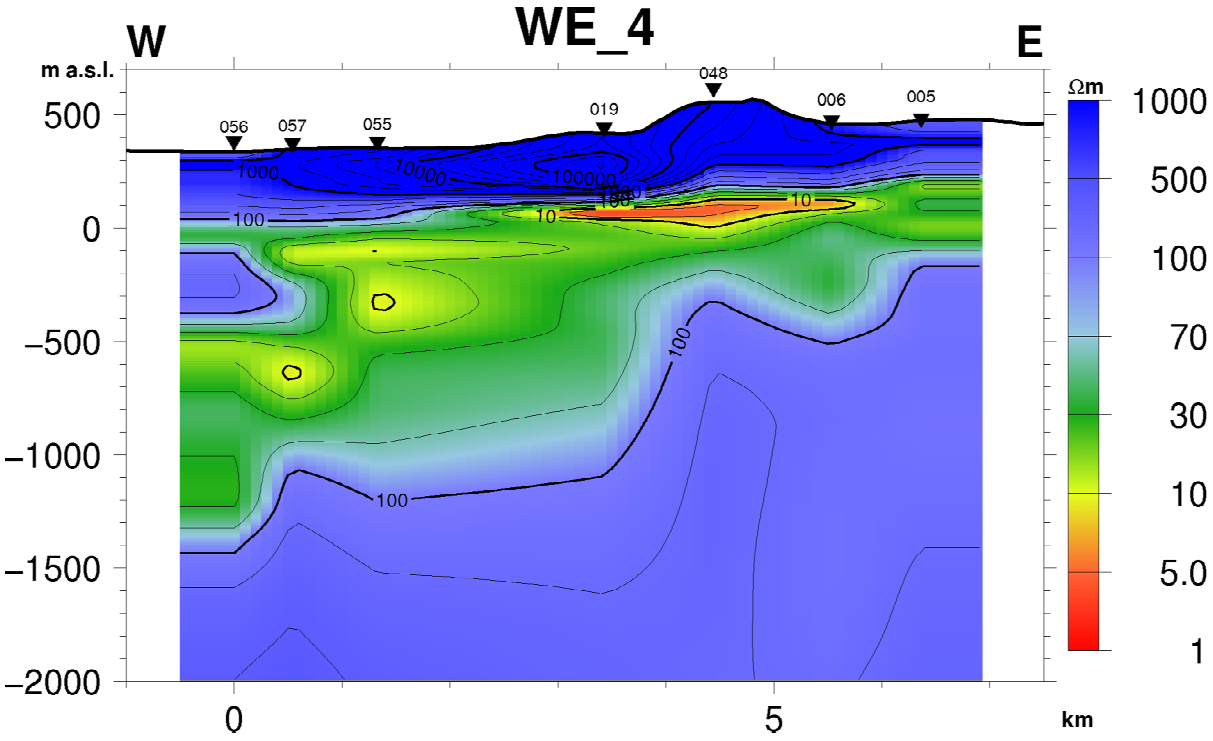

FIGURE 22: Resistivity profile WE_4 based on 1D joint inversion of TEM and MT data, reaching down to 2,000 m b.s.l.

6.6 MT iso-resistivity maps

Resistivity map at sea level. There are two distinct low-resistivity bodies observed at sea level that are at 350 m depth from the surface (Figure 23). These two anomalies are part of the low-resistivity smectite-zeolite zone reaching the surface, visible in Figure 23.

Resistivity map at 500 m b.s.l. is shown in Figure 24. Two high-resistivity anomalies align themselves in a NW-SE orientation at about 850 m depth below the surface, representing the resistive core. The low resistivity at the edges of the map shows the low-resistivity cap as it tilts down away from the centre of the geothermal system at Bóndhólsskard.

Resistivity map at 1000 m b.s.l. (Figure 25). At the depth of 1400 m from the surface, the high-resistivity core correlating to the chlorite-epidote alteration zone is clearly mapped, trending in an east-west direction (Figure 25).

Resistivity map at 3000 m b.s.l. (Figure 26). Two low-resistivity anomalies appear in the central part of the area, close to Bóndhólsskard to the east and Stórihver in the west. This could be an indication of a deeper conductor related to the heat source. The low-resistivity layer is clearly mapped at 5000 m b.s.l. and extends to the north of the area (Figure 27).

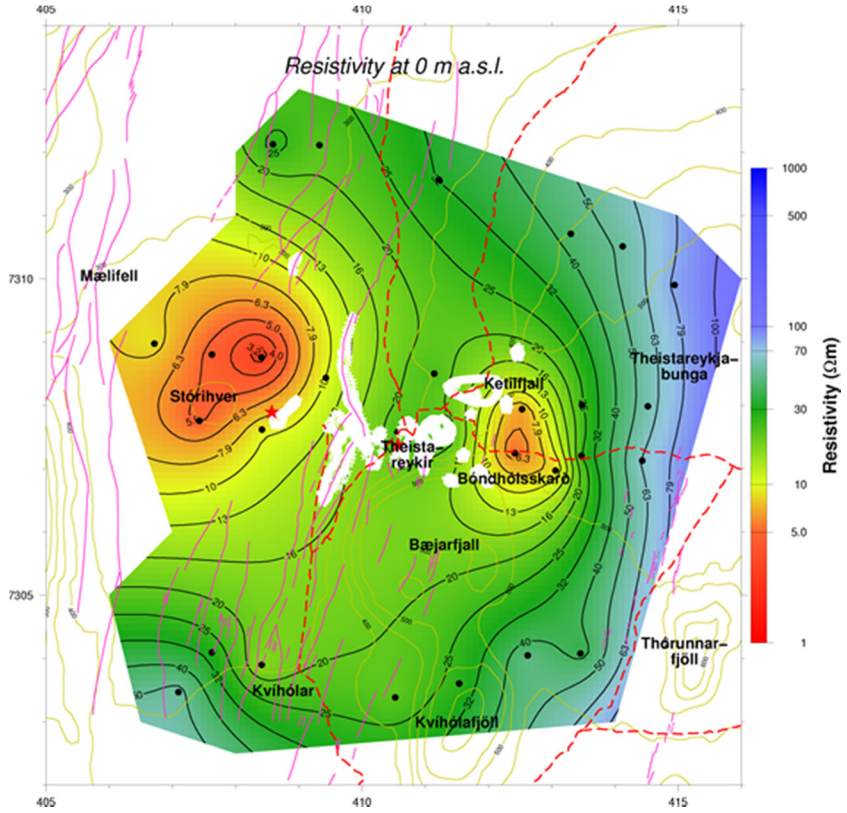

FIGURE 23: Resistivity in the Theistareykir area based on 1D inversion of TEM and MT data at sea level; black dots are MT soundings, magenta (dark) lines are geological fractures, white shades are surface manifestations, red (dark) stars are wells and red (dark) dashed lines are roads

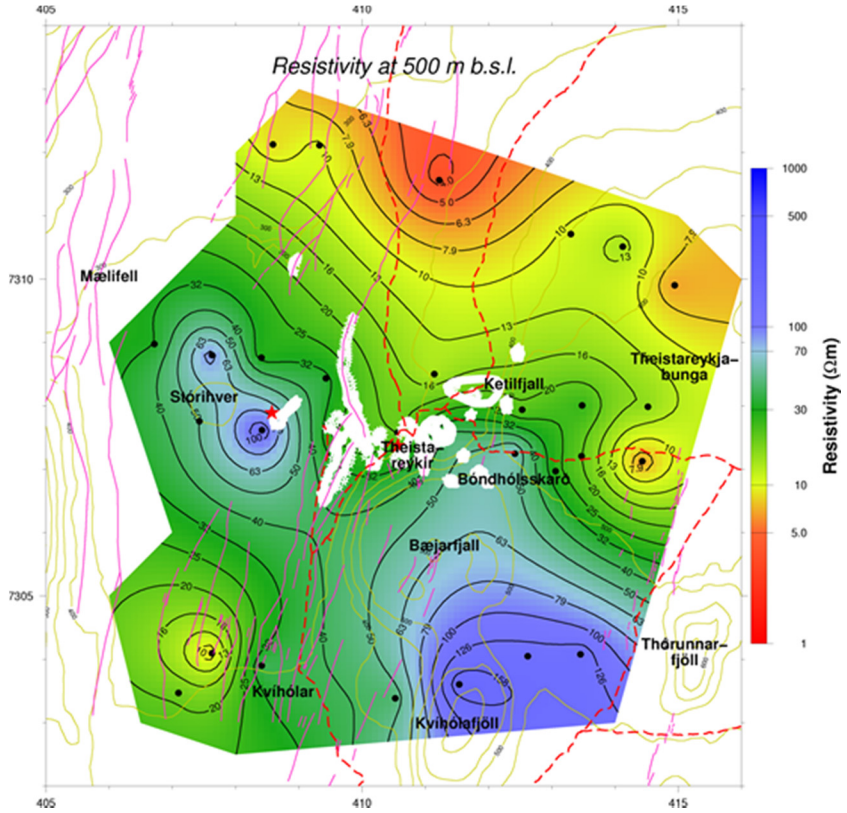

FIGURE 24: Resistivity in the Theistareykir area based on 1D inversion of TEM and MT at 500 m b.s.l.; other symbols are explained in the caption of Figure 23

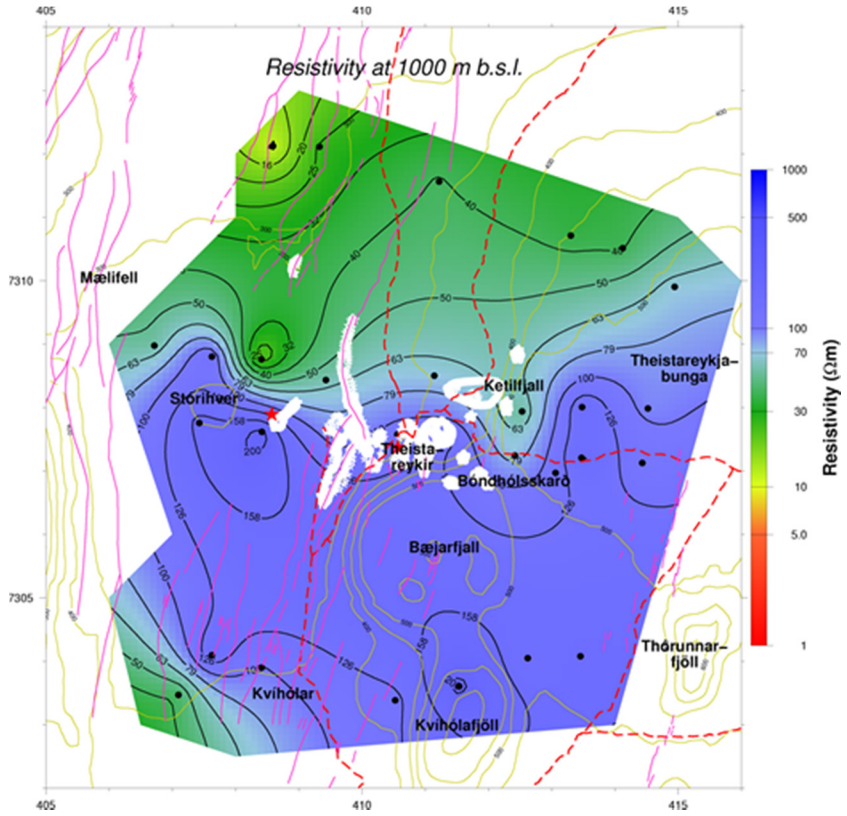

FIGURE 25: Resistivity in the Theistareykir area based on 1D inversion of TEM and MT at 1000 m b.s.l.; other symbols are explained in the caption of Figure 23

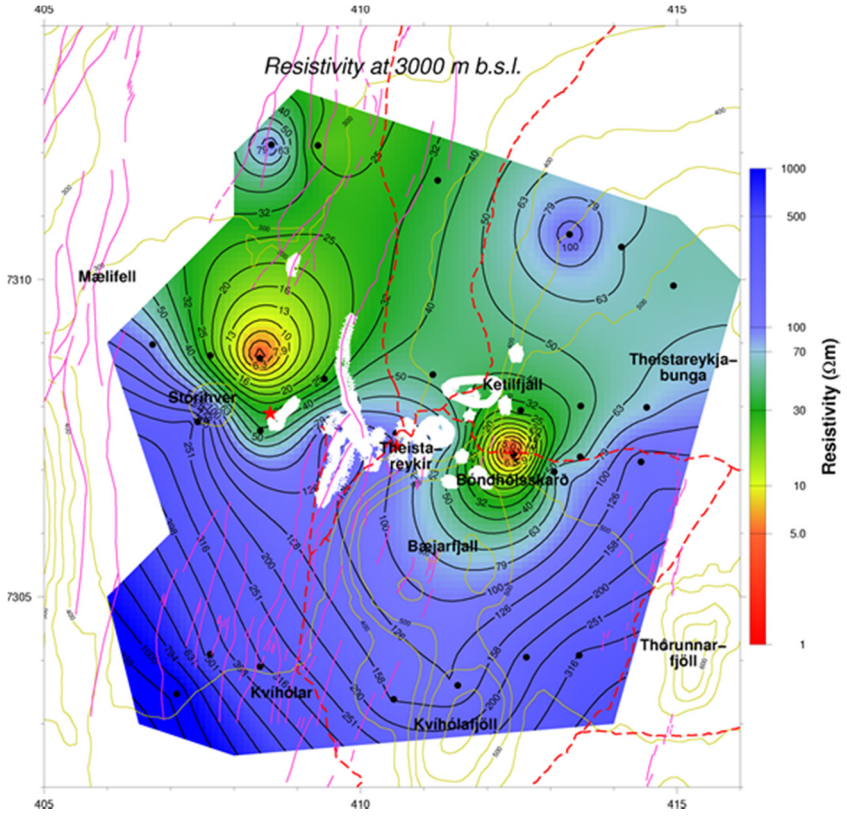

FIGURE 26: Resistivity in the Theistareykir area based on 1D inversion of TEM and MT at 3000 m b.s.l.; other symbols are explained in the caption of Figure 23

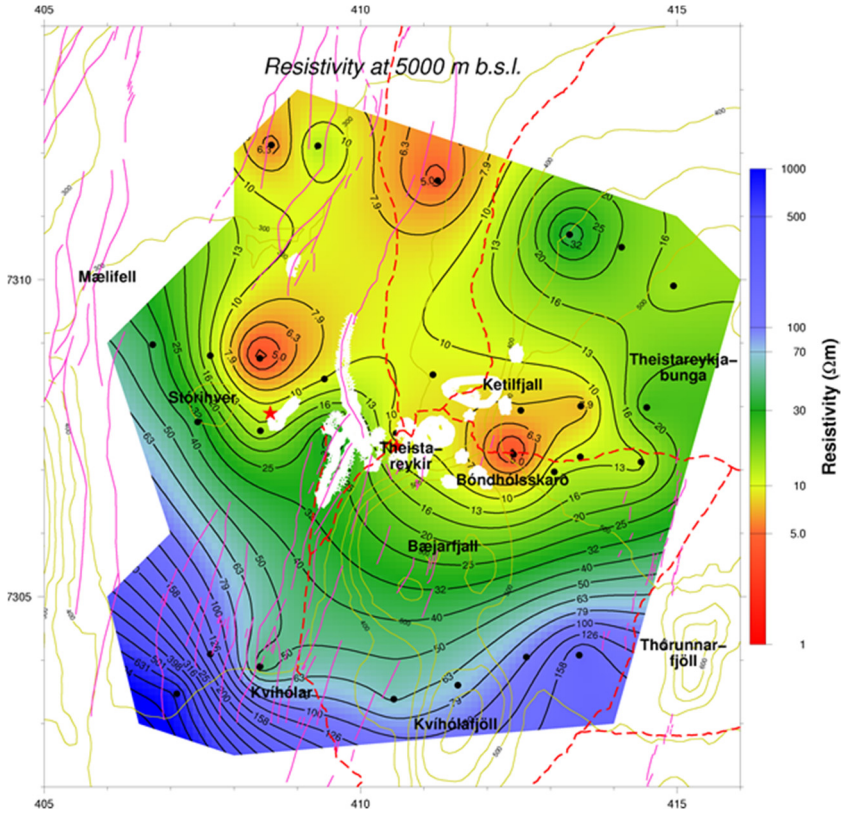

FIGURE 27: Resistivity in the Theistareykir area based on 1D inversion of TEM and MT at 5000 m b.s.l.; other symbols are explained in the caption of Figure 23

7. COMPARISON OF RESISTIVITY RESULTS WITH HYDROTHERMAL ALTERATION AND TEMPERATURE FROM BOREHOLES IN THE THEISTAREYKIR AREA

Figure 28 shows a comparison of the subsurface resistivity structure with the available borehole alteration and temperature logs. Resistivity cross-section WE_3 is within 50-100 m of boreholes ThG-05 and ThG-08 (Figure 9). These are directional wells that were drilled to an average of 2 km depth. However, for borehole ThG-08, only temperature information was available for comparison.

Figure 28 shows a very good correlation between the resistivity and temperature for well ThG-05, as well as temperature for well ThG-08.The low-resistivity layer correlates well with the smectite-zeolite alteration zone in borehole ThG-05, reaching the surface, and borehole temperature for both boreholes at 200°C. The chlorite-epidote alteration zone in the borehole also correlates well with the high-resistivity of the cross-section and formation temperatures of 250 and 300°C for wells ThG-05 and ThG-08, respectively.

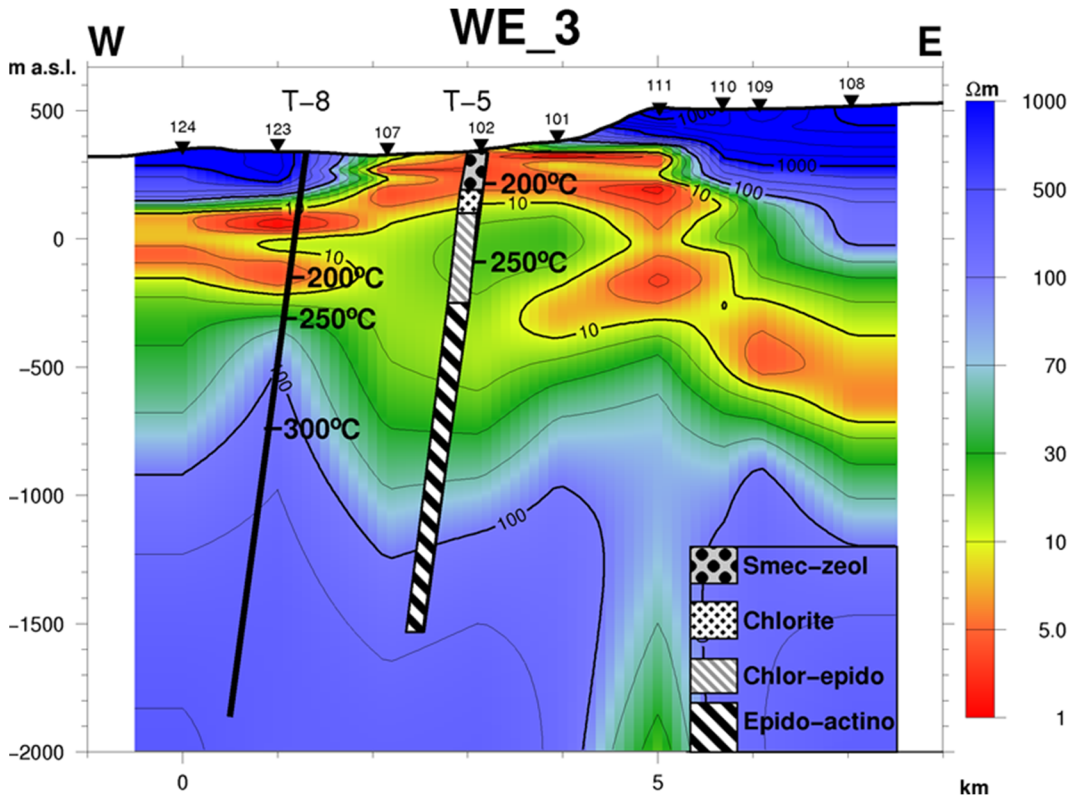

FIGURE 28: Resistivity cross-section WE_3, temperature logs in boreholes and alteration zoning

8. CONCLUSIONS AND DISCUSSION

Results of joint inversion of TEM and MT data of two profiles (WE_3 and WE_4), based on cross-sections and iso-resistivity maps generated with additional two profiles (WE_1 and WE_2, Suriyarachchi, 2012), revealed the following resistivity layers:

- A high-resistivity layer near the surface (> 1000 Ωm) down to a depth of 200-300 m, correlating to the un-altered rocks close to the surface.

- Underneath the high-resistivity layer is a conductive layer or cap (< 10 Ωm) which reaches the surface, where there are evident numbers of surface manifestations and alterations. This

conductive layer correlates to the smectite and zeolite zone and surface conduction in clay minerals dominates in this zone.

- Below the conductive layer is a highly resistive core (> 100 Ωm) that is evident in both cross-sections and emerges at 500 m b.s.l. in iso-resistivity maps. The existence of the resistive core indicates reservoir temperatures exceeding 250°C, correlating to the chlorite-epidote zone.

- A low-resistivity anomaly (< 10 Ωm), possibly a deep conductor, is evident on cross-section WE_3 at depth of 4.5-5 km and emerges on iso-resistivity maps at 5000 m b.s.l. This low-resistivity anomaly lies northeast of Stórihver and north of Bóndhólsskard.

There is a good correlation between the subsurface resistivity and borehole alteration/temperature logs. The smectite-zeolite zone is found where the subsurface resistivity is low or reaching the surface, while the resistive core correlates with the deep alteration zone consisting of chlorite-epidote.

From the analysis of the resistivity layers of Theistareykir geothermal area and their comparison to borehole hydrothermal alteration/temperature logs, it was confirmed that resistivity methods (TEM and MT) are a powerful geophysical prospecting method in high-temperature geothermal areas in delineating geothermal resources.

ACKNOWLEDGEMENTS

I would like to express my thanks to Dr. Ingvar Birgir Fridleifsson, director UNU-GTP, and Mr. Lúdvík S. Georgsson, deputy director, for giving me the opportunity to participate in this six months course. Special thanks to my supervisors, Mr. Gylfi Páll Hersir and Mr. Andemariam Teklesenbet, together with my co-supervisor Mr. Knútur Árnason, for their assistance and daily guidance during the study period and most especially during data processing, analysis and report writing. My sincere gratitude to Ms. Ragna Karlsdóttir for her critical review of the manuscript. Also to Ms. Thórhildur Ísberg, Mr. Ingimar G. Haraldsson, Ms. Málfrídur Ómarsdóttir and Mr. Markús A.G. Wilde for their routine assistance during the training.

I extend my gratitude to my employer, the Ministry of Energy and Mineral Development, Department of Geological Survey and Mines for granting me permission to attend this six months course. Special thanks to all the UNU Fellows for their valuable discussions on various disciplines of geothermal exploration and for their friendship. My sincere appreciation to my family for their patience and support during the course of the programme. And lastly, but most of all, to the Almighty God, who made everything possible.

REFERENCES

Archie, G.E., 1942: The electrical resistivity log as an aid in determining some reservoir characteristics. *Tran. AIME, 146,* 54-67.

Ármannsson, H., Gíslason, G., and Torfason, H., 1986: Surface exploration of the Theistareykir high-temperature geothermal area, with special reference to the application of geochemical methods. *Applied Geochemistry*, 1, 47-64.

Árnason, K., 2006a: *TemX Short manual*. ÍSOR – Iceland GeoSurvey, Reykjavík, internal report, 17 pp.

Árnason, K., 2006b: *TEMTD, a programme for 1D inversion of central-loop TEM and MT data. Short manual*. ÍSOR – Iceland GeoSurvey, Reykjavík, manual, 17 pp.

Árnason K., Eysteinsson, H., and Hersir, G.P., 2010: Joint 1D inversion of TEM and MT data and 3D inversion of MT data in the Hengill area, SW Iceland. *Geothermics*, *39,* 13–34.

Árnason, K., Flóvenz, Ó., Georgsson, L.S., and Hersir, G.P., 1987a: Resistivity structure of high-temperature geothermal systems in Iceland. *International Union of Geodesy and Geophysics (IUGG) XIX General Assembly, Vancouver Canada, Abstracts V,* 477.

Árnason, K., Haraldsson, G.I., Johnsen, G.V., Thorbergsson, G., Hersir, G.P., Saemundsson, K., Georgsson, L.S., Rögnvaldsson, S.Th., and Snorrason, S.P., 1987b*: Nesjavellir-Ölkelduháls, surface exploration 1986*. Orkustofnun, Reykjavík, report OS-87018/JHD-02 (in Icelandic), 112 pp+maps.

Árnason, K., Karlsdóttir, R., Eysteinsson, H., Flóvenz, Ó.G., and Gudlaugsson, S.Th., 2000: The resistivity structure of high-temperature geothermal systems in Iceland. *Proceedings of the World Geothermal Congress 2000, Kyushu-Tohoku, Japan*, 923-928.

Bahati, G., 2011: Status of geothermal exploration and development in Uganda. *Paper presented at "Short Course VI on Exploration for Geothermal Resources", organized by UNU-GTP, GDC and KenGen, Lake Bogoria and Lake Naivasha, Kenya,* 14 pp.

Dakhnov, V.N., 1962: Geophysical well logging. *Q. Colorado Sch. Mines, 57-2*, 445 pp.

DeGroot-Hedlin, G., 1991: Removal of static shift in two dimensions by regularized inversion. *Geophysics*, *56,* 2102-2106.

Eysteinsson, H., 1998: *TEMRESD, TEMMAP and TEMCROSS plotting programs*. ÍSOR – Iceland GeoSurvey, unpublished programs and manuals.

Flóvenz, Ó.G., Hersir, G.P., Saemundsson, K., Ármannsson, H., and Fridriksson, T., 2012: Geothermal energy exploration techniques. In: Sayigh, A., (ed.) *Comprehensive renewable energy*, *Vol. 7,* Elsevier, Oxford, 51-95.

Gautason, B., Gudmundsson, Á., Hjartarson, H., Blischke, A., Mortensen, A.K., Ingimarsdóttir, A., Gunnarsson, H.S., Sigurgeirsson, M.Á., Árnadóttir, S., and Egilson, Th., 2010: Exploration drilling in the Theistareykir high-temperature field, NE-Iceland: Stratigraphy, alteration and its relationship to temperature strucure. *Proceedings of the World Geothermal Congress 2010, Bali, Indonesia,* 5 pp.

Grönvold, K., and Karlsdóttir, R., 1975: *Theistareykir. An interim report on the surface exploration of the geothermal area*. Orkustofnun, Reykjavík, report JHD-7501 (in Icelandic), 37 pp.

Gudmundsson, Á., Gautason, B., Thórdarson, S., Egilson, T., and Thórisson, S., 2002: *Exploration drilling at Theistareykir. Well Th.G-1. 3rd stage: Drilling of production part to 1953 m depth*. Orkustofnun, Reykjavík, report OS-2002/079 (in Icelandic), 59 pp.

Hersir, G.P., 2012: *Resistivity of rocks*. UNU-GTP, Iceland, unpublished lecture notes.

Hersir, G.P., and Árnason, K., 2009: Resistivity of rocks. *Paper presented at "Short Course on Surface Exploration for Geothermal Resources", organized by UNU-GTP and LaGeo, Santa Tecla, El Salvador,* 8 pp.

Hersir, G.P., and Björnsson, A., 1991: *Geophysical exploration for geothermal resources. Principles and applications*. UNU-GTP, Iceland, report 15, 94 pp.

Kahwa, E., 2012: Appendices to the report *"Geophysical exploration of high-temperature geothermal areas using resistivity methods – case study: Theistareykir area, NE-Iceland."* UNU-GTP, Iceland, report 14 appendices, 28 pp.

Karlsdóttir, R., Eysteinsson, H., Magnússon, I.Th., Árnason, K., and Kaldal, I., 2006: *TEM soundings at Theistareykir and Gjástykki 2004-2006*. ÍSOR – Iceland GeoSurvey, Reykjavík, report ÍSOR-2006/028 (in Icelandic), 88 pp.

Keller, G.V., and Frischknecht, F.C., 1966: *Electrical methods in geophysical prospecting*. Pergamon Press Ltd., Oxford, 527 pp.

Manzella, A., 2007: *Geophysical methods in geothermal exploration*. Italian National Research Council, International Institute for Geothermal Research, Pisa. 40 pp. Web page: *http://cabierta.uchile.cl/revista/12/articulos/pdf/A_Manzella.pdf* .

Ogawa, Y., and Ushida, T., 1996: A two-dimensional magnetotelluric inversion assuming Gaussian static shift. *Geophys. J. Int., 126*, 69-76.

Quist, A.S., and Marshall, W.L., 1968: Electrical conductances of aqueous sodium chloride solutions from 0 to 800°C and at pressures to 4000 bars. *J. Phys. Chem., 72,* 684-703.

Saemundsson, K., 2007: *The geology of Theistareykir.* ÍSOR – Iceland GeoSurvey, Reykjavík, report ÍSOR-07270 (in Icelandic), 23 pp.

Sternberg, B.K., Washburn, J.C., and Pellerin, L., 1988: Correction for the static shift in magnetotellurics using transient electromagnetic soundings. *Geophysics*, *53-11*, 1459-1468.

Suriyaarachchi, N.B., 2012: Joint 1D inversion of MT and TEM resistivity data from the Theistareykir high-temperature geothermal area, NE-Iceland and comparison with alteration and temperature logs from boreholes. Report 32 in: *Geothermal training in Iceland 2012*. UNU-GTP, Iceland, 793-822.

Teklesenbet, A. B., 2012: *Multidimensional inversion of MT data from Alid Geothermal area, Eritera; comparison with geological strucures and identification of a geothermal reservoir.* University of Iceland, MSc thesis, UNU-GTP, Iceland, report 1, 120 pp.

Ussher, G., Harvey, C., Johnstone, R., and Anderson, E., 2000: Understanding the resistivities observed in geothermal systems. *Proceedings of the World Geothermal Congress 2000, Kyushu-Tohoku, Japan, 51915-1920.*

Vozoff, K., 1972: The magnetotelluric method in the exploration of sedimentary basins. *Geophysics, 37,* 98-141.

Vozoff, K., 1991: The magnetotelluric method. In: Nabighian, M.N (ed), *Electromagnetic methods in applied geophysics*, *Vol. II,* 641-711.